(IJNCAA)

ISSN 2220-9085(ONLINE)
ISSN 2412-3587(PRINT)

INTERNATIONAL JOURNAL OF

New Computer Architectures and their Applications

Volume 9, Issue 1,
2019

SDIWC

www.sdiwc.net

International Journal of
NEW COMPUTER ARCHITECTURES AND THEIR APPLICATIONS

Overview

The SDIWC International Journal of New Computer Architectures and Their Applications (IJNCAA) is a refereed online journal designed to address the following topics: new computer architectures, digital resources, and mobile devices, including cell phones. In our opinion, cell phones in their current state are really computers, and the gap between these devices and the capabilities of the computers will soon disappear. Original unpublished manuscripts are solicited in the areas such as computer architectures, parallel and distributed systems, microprocessors and microsystems, storage management, communications management, reliability, and VLSI.

One of the most important aims of this journal is to increase the usage and impact of knowledge as well as increasing the visibility and ease of use of scientific materials, IJNCAA does NOT CHARGE authors for any publication fee for online publishing of their materials in the journal and does NOT CHARGE readers or their institutions for accessing the published materials.

Publisher

The Society of Digital Information and Wireless Communications
20/F, Tower 5, China Hong Kong City, 33 Canton Road, Tsim Sha Tsui, Kowloon, Hong Kong

Further Information

Website: http://sdiwc.net/ijncaa, Email: ijncaa@sdiwc.net,
Tel.: (202)-657-4603 - Inside USA; 001(202)-657-4603 - Outside USA.

The issue date is Mar. 2019.

IJNCAA
ISSN 2220-9085 (Online)
ISSN 2412-3587 (Print)
Volume 9, Issue No. 1
2019

CONTENTS

ORIGINAL ARTICLES

International Journal of
NEW COMPUTER ARCHITECTURES AND THEIR APPLICATIONS

The *International Journal of New Computer Architectures and Their Applications* aims to provide a forum for scientists, engineers, and practitioners to present their latest research results, ideas, developments and applications in the field of computer architectures, information technology, and mobile technologies. The IJNCAA is published four times a year and accepts three types of papers as follows:

1. **Research papers**: that are presenting and discussing the latest, and the most profound research results in the scope of IJNCAA. Papers should describe new contributions in the scope of IJNCAA and support claims of novelty with citations to the relevant literature.
2. **Technical papers**: that are establishing meaningful forum between practitioners and researchers with useful solutions in various fields of digital security and forensics. It includes all kinds of practical applications, which covers principles, projects, missions, techniques, tools, methods, processes etc.
3. **Review papers**: that are critically analyzing past and current research trends in the field.

Manuscripts submitted to IJNCAA **should not be previously published or be under review** by any other publication. Plagiarism is a serious academic offense and will not be tolerated in any sort! Any case of plagiarism would lead to life-time abundance of all authors for publishing in any of our journals or conferences.

Original unpublished manuscripts are solicited in the following areas including but not limited to:

- Computer Architectures
- Parallel and Distributed Systems
- Storage Management
- Microprocessors and Microsystems
- Communications Management
- Reliability
- VLSI

International Journal of New Computer Architectures and their Applications (IJNCAA) 9(1): 1-10
The Society of Digital Information and Wireless Communications, 2019 ISSN 2220-9085 (Online); ISSN 2412-3587 (Print)

Forecasting of HOSR for Different Mobile Carriers in Kano Using Conventional and Intelligent Techniques

S. B. Abdullahi* and M. S. Gaya**
*Department of Physics, College of Natural and Pharmaceutical Sciences, Bayero University Kano. PMB 3011, Kano-Nigeria 700241.
**Department of Electrical Engineering, Faculty of Engineering, Kano University of Science & Technology, Wudil.
sba_elt.bch@outlook.com

ABSTRACT

Handover is the key concept to achieve mobility and its success rate determine the subscriber satisfaction. It is a critical process and if performed incorrectly can result in the loss of calls. Therefore, reliable and accurate prediction of Handover Success Rate (HOSR) is very essential. The available models did not well capture the impact of selected inputs dataset of HOSR. The comparison between the conventional technique-Hammerstein-Wiener (HW) and intelligent technique-Adaptive Neuro-fuzzy Inference System models in forecasting HOSR are considered. Seven months log files were generated from four active GSM-1800 networks in Kano Metropolis with the aid of TEMS Pocket. The collected data were embedded in the construction of the trained networks. The results depicted that Conventional technique is superior to the intelligent technique for predicting HOSR. The performance of the linguistic models was tested using MAPE, where ANFIS achieved 0.3358, 0.2834, 0.0092, 0.9519: and HW achieved 0.0000, 0.0683, 0.1810, 0.0568 and with RMSE, ANFIS achieved 50.5677, 39.4984, 6.8271, 139.6244: and HW achieved 0.0000, 9.4974, 134.4543, 45.6185 for P, Q, R and S respectively. Thus, the Conventional technique would be suitable in forecasting HOSR in Kano or any environment with similar network deployment.

KEYWORDS
Handover, ANFIS, HW, HOSR, MAPE, RMSE, FPE.

1 INTRODUCTION

The innovations in cellular networks are emerging subject to the demand of users. Global System for Mobile Communications (GSM) is one of the most popular cellular networks that enabled voice telephony to go wireless [1]-[2]. Many countries have implemented the 4th generation (4G) mobile network whereas others are still with the 2nd generation (2G) GSM network which is the case of Nigeria. GSM network still accounted for more than 70% of the voice calls and other voice telephony services in Nigeria, with the following four fully functional GSM carriers. Because of the legal issues and for the purpose of this paper the network names are anonymize to P, Q, R and S. User mobility during call can result in a change of BTS (Base Transceiver Station). The effect of mobility is handover. Mobility needs special handling of Quality of Service (QoS) protocols and techniques [3]. Handover is a method that ensures retention of the ongoing call into another cell [4]. It is a critical process and if performed incorrectly can result in the loss of calls. It is often initiated either by a deterioration in quality of the signal in the current channel or crossing a cell boundary [4]-[5]. As in [6] explained how the average signal strength of base transceiver station one (SBS1) is decreasing as the mobile station (MS) is moving away from it, while the average signal strength of base transceiver station two (SBS2) is increasing as the MS is approaching it, as given in figure 1 below. Another problem associated with poor handling of handover is overloading of the system processor which can bring about incessant system breakdown which also leads to revenue loss. The handover process is expected to be successful, imperceptible and less frequent. Unsuccessful handover can be very annoying to subscribers. It terminates established connections forcefully leading to dropped calls and degraded QoS [4]. High handover requests catastrophically increase traffic load and will degrade QoS, increase call set up time and call blocking probabilities. Efficient Handover Success Rate (HOSR) techniques minimized cost and enhance the capacity and QoS, maintain cell borders and appropriate traffic balancing, and minimize number of handovers and global interference. A

precise and accurate forecast of HOSR in the 2G network is an essential task for a network carrier, as the upgrade path for network infrastructure needs multiple month time to be implemented [7]. Thus, necessitated the need of having an accurate and reliable tool in forecasting the behavior of HOSR. The major challenge of forecasting HOSR in cellular network is the non-linearity behavior of the network parameters, and HOSR forecasting in mobility management is a complicated task since the demand is affected directly by various factors associated with the QoS protocols and the system overloading. Therefore, this research took into consideration parameters that are primarily associated with these challenges. HOSR is the Key Performance Indicator connected to network Retainability [8] that determines the success rate of subscribers' satisfaction. The possible reasons for poor HOSR are congestion, link connection, incorrect handover relations, incorrect locating parameter setting, bad radio coverage, high interference, co-channel or adjacent interference etc. [8]. HOSR can be found using equation (4) below. The handover failures occur when the quality of the connection is less than the threshold level [6]-[9]. A minimum acceptable D$minimum$ value between -85dBm to -105dBm signals is considered for voice quality. A stronger signal level, $Dthreshold$ is used to define the threshold at which handover is initiated as in Figure 1. A differential $\Delta handover$ is used by the Mobile Switching Centre (MSC) to control handover procedure. If $\Delta handover$ is too large, too many hand-overs occur and the MSC is over engaged. If $\Delta handover$ is too small, there may be insufficient time to complete a handover before a call is lost due to weak signal level [9]:

$$\Delta_{handover} = D_{threshold} - D_{minimum} \qquad (1)$$

Despite substantial existing literatures, various open issues remain, as in [5] analyzed handover using the live GSM data, different issues, findings, trials and improvements have been summarized and possible recommendations were listed and correlated it to the practical aspects of handover, but this work did not mention any improvements made on the existing data. In another work [10] designed an approach to maximize handover performance success rate and enhancement of voice quality samples for a GSM Cellular Network, where 93 BTS (Base Transceiver Station) sites in India City were simulated, the obtained results are very promising over existing system and 11% and 12% improvements were made in National Busy Hour (NBH) HOSR and during Bouncing Busy Hour (BBH) HOSR respectively. Henceforth voice quality DL and UL in BBH period were also improved by 17% and 14% respectively, which according to the authors are directly linked with customer satisfaction and revenue of the company, but much attention was not given to the NBH HOSR. Likewise, [4] analyzed and optimized intercell handover dynamics in a GSM Network of Airtel Kano, where three months call record sample data was recorded and standard mathematical relationships of HOSR and other relevant KPIs were developed and the cells were found performed below NCC target. An optimal solution was provided using dynamic cut-off priority channel allocation scheme on a JAVA Variant NETBEANS 6.1 platform. The result showed that handover failure rate was reduced by an average of 90% for varying loads and a coefficient correlation of 0.9122 was calculated using MATLAB. In [11] compared and analyzed ANN and ANFIS methods in forecasting HOSR, the models were developed using both MATLAB and MS Excel sheet and validated using 15% of actual data, ANN was concluded as a superior method in predicting HOSR due to it less RMSE compared to ANFIS method, but this work predicted only the load variables of Etisalat and performance validation of the forecasted models were not carried out in the research. [12] Presented the design and implementation of a Fuzzy Logic multi-criteria handoff algorithm based on signal strength, path-loss and traffic load of base stations and the received signal to interference ratio as to balance traffic in all the neighboring sites at any time, but the evaluation of the model is not carried out and the model is not compared with any other available models. Likewise, [13] developed a performance model for handover manageability in CDMA networks, the training and validation phase of the networks confirmed that the soft handover is very inefficient which led to the loss of calls and QoS degradation, according to the authors view if this proposed model is implemented on active networks, enhanced QoS will be achieved, but the

work is limited to only one CDMA carrier. Based on the available literature, and the limitations of the various research outlines above, as in [11] forecasted HOSR based on the ANN and ANFIS models respectively, but HW model has not been addressed for HOSR, this paper forecasted the linguistic models of HOSR using both intelligent and conventional techniques, and the work compared the performance, suitability and robustness of the conventional and intelligent techniques in forecasting HOSR in GSM network. The models were trained using four GSM carriers load variables and the comparison of the various models were provided, therefore the research validated that the conventional technique outperformed the intelligence technique.

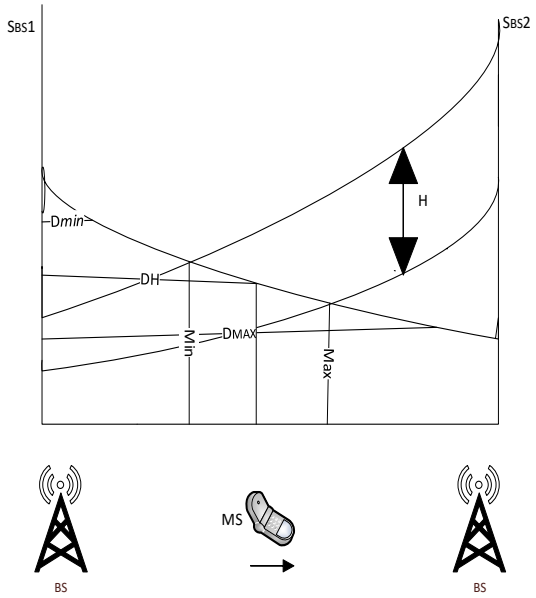

Figure 1. Handover between two Base Transceiver Stations (BSs) modified in [6].

2 HOSR AFFECTED PARAMETERS

2.1 Traffic Channels (TCH): these are logical channels over which user information are exchanged between mobile users during a connection. TCH Congestion Rate provides the percentage of attempts to allocate a TCH call setup that was blocked in a cell [14]. In a properly dimensioned network, the value of this statistics should not be more than 2% [8]. The reasons for this block are high increase in traffic demand, bad dimensioning, high mean holding time, low hand over activity and high antenna position etc. This index can be deduced using [8]:

$$\text{TCH Cong.} = \frac{(CC11)}{(CC12)} \times 100\% \qquad (2)$$

Where CC11 counts number of assignment failures when no TCH available, and CC12 counts number of normal assignment requests for TCH establishment.

2.2 Standalone Dedicated Control Channel (SDCCH): This channel is always used when a traffic channel has not been assigned and is allocated to a mobile station only as long as control information is being transmitted. It measures the ease with which a call can be setup, the ease to recharge an account, send SMS, location update, paging etc. Reasons for poor SDCCH were too high timing advance, congestion, low signal strength on downlink or uplink, false accesses due to high noise floor, it is given by [8]:

$$SDCCH\ Cong.rate = \frac{1-CSSR}{CC12} \times 100\% \quad (3)$$

Where CSSR is the call setup success rate and CC12 is the TCH assignment rate.

2.3 Hand over Success Rate (HOSR): This metric can be obtained by taking into account percentage of successful handovers over handover attempts [14]. The possible reasons for poor HOSR are congestion, link connection, incorrect handover relations, incorrect locating parameter setting, bad radio coverage, high interference, co-channel or adjacent etc. This can be found using [8]:

$$HOSR = \frac{[(CC7+CC8)]}{[(CC9+CC10)]} \times 100\% \quad (4)$$

Where CC7 counts number of incoming successful handovers, and CC8 counts number of outgoing successful handovers. CC9 counts number of outgoing HO requests while CC10 counts number of incoming HO requests.

2.4 Handover Success Rate (Intra_HSR): this happen during ongoing call, the Mobile Station (MS) needs to change the frequency or time slot being used due to interference or some other reasons, the MS remains attached to the same BS, but changes the frequency or timeslot [8]-[14].

2.5 Root Mean Square Error (RMSE): This is obtained by calculating the average of the square root of forecast errors, it however measures how

well the response of the model fits the estimation data and determine the size of the error [15]-[16];

$$RMSE = \sqrt{\frac{\sum(x_i - y_i)^2}{N}} \quad (5)$$

2.6 Mean Absolute Percentage Error (MAPE): This determine the effect of the magnitude of the actual values, however it measures how accurate the forecast system is and assessed the size of the error [15]-[16];

$$MAPE = \frac{100\%}{N} * \sum_{i=1}^{N} \left|\frac{x_i - y_i}{x_i}\right| \quad (6)$$

Where x_i is the measured value, y_i is the forecast value and N gives the number of samples.
For a highly accurate model the value of MAPE should be less than 10% and for good forecast should be 11% to 20%, while for inaccurate forecast this value started from 51% to above [16].

2.7 Loss Function (Loss fcn or V): This compare the predicted output with the measured output. The closer the predicted and the measured outputs are, the smaller the criterion V, therefore the more accurate the model will be. This value need to be lowest for highly accurate model [17].

$$V = \frac{1}{N}\sum_{k=1}^{N} \varepsilon^2\,(k, \theta, \eta) \quad (7)$$

where N is the number of measurements, $\varepsilon\,(k, \theta, \eta)$ is the prediction error.

2.8 Final Prediction Error (FPE): This provides a measure of model quality by simulating the condition where the model is tested on a different data set and it is given by [17]-[19]:

$$FPE = V\left[\frac{1+{}^{\varepsilon}/_{N}}{1-{}^{\varepsilon}/_{N}}\right] \quad (8)$$

2.9 Percentage Best Fit (Fit %): This can be obtained from the comparison between the estimated data and the validation data, thus it is given by [17]-[18];

$$Fit\,\% = 100 \times \left(1 - \frac{norm(y^* - x_i)}{norm(x_i - x)}\right) \quad (9)$$

where y^* is the simulated output, x_i is the estimated data and x is the mean of the output.

3 MATERIALS AND METHODS

Neuro-Fuzzy is developed out of the linguistic combination of neural network and fuzzy logic to solve the inherent limitations of the individual method. Adaptive Neuro-Fuzzy Inference System (ANFIS) is one of the classified hybrids neuro-fuzzy technique with universal acceptability since development. The technique yields an effective result for non-linear mapping [20]-[19]. ANFIS incorporate nodes and five layers. As depicted in Fig. 2 [22] the circular nodes are fixed while the square nodes are adaptive with built-in variables to be updated while supervised learning. Hammerstein-Wiener (HW) model is developed out of the linguistic combination of Wiener model and Hammerstein model to form one block of model. HW is a block-structured nonlinear model, that consists of static nonlinear model with linear time invariant (dynamic) block system [17]-[21]. HW finds application in digital communication systems, control engineering etc.
The general structure of the HW model is given by Figure 3, where u (t) is the inputs to the nonlinear block of the system, w (t) is the outputs from the nonlinear block of the system, x (t) is an internal variable that defines the input and output of the linear block, y (t) is the output of the system, f is the nonlinear function that transforms input data as w (t), n is the total number of inputs, B/F is the linear transfer function that transforms w (t) as x (t), h is the nonlinear function that maps the output of the linear block x (t) to the system output y (t). B and F are the numerator and denominator similar to polynomials in a linear output-error model. Henceforth, *nu* and *ny* are the inputs and ouputs, therefore with this function, the linear block is a transfer function matrix containing the following entries [17]-[21]:

$$B^{j,i}(q)F^{j,i}(q)$$

where j = 1,2,...,ny and i = 1,2,...,nu.
Using Figure 3 above, the following equations were generated as the HW general equations:

$$w(t) = f\big(u(t)\big) \quad (10)$$

$$x(t) = \sum_{i}^{n} \frac{B^i(q)}{F^i(q)}\,\mathrm{w}\big(t - n_y\big) \quad (11)$$

$$y(t) = h\big(x(t)\big) \quad (12)$$

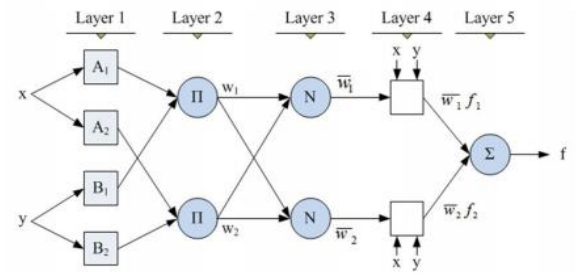

Figure 2. The ANFIS Structure with 2 Ruled Sugeno Type

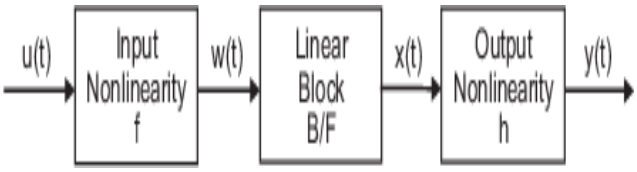

Figure 3. The general structure of the HW [21].

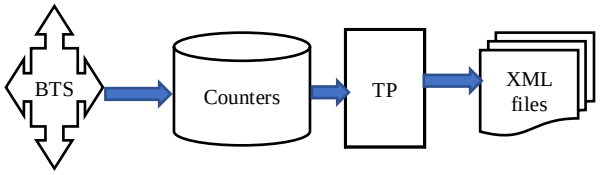

Figure 4. Data generation/Experimental setup

Where BTS: Base Transceiver Station, TP: W995 TEMS Pocket, XML: extensible markup language.

3.1 Data Extraction and Model Constructions

The data was generated using W995 Ericson Test Phone with built-in (Terrestrial/Transmission Eco mobile System, TP). TP is a convenient and powerful product for verification, monitoring and troubleshooting of mobile networks and also for basic cell-planning tasks [23]. TP collects measurements and event data for immediate monitoring or for processing by other tools at a later time. It can capture data in areas that are difficult to cover during traditional drive-testing. The tool provides options to perform indoor-environment measurements quickly and easily and it has an added powerful scanner that places extensive data-gathering capabilities in the palm of the user's hand [23]-[24]. The log files generated were written in XML files which was later computed and converted into an Excel files, as depicted in figure 4, these files may likely contain corrupted or missing values, outliers etc. which was impossible to reprogram a live system, due to reliability and security reasons. The weighted average of the selected GSM load variables was considered, due to it gives more representative and stable values. Therefore 90% of the data were fed into the training process at random, while 10% was selected for testing phase. The Intelligent technique model was developed based on Adaptive Neuro-fuzzy Inference System (ANFIS) using MATLAB (R2013b) command "genfis1". The construction was set three trapezoidal membership function (mf) to each input and generated eighty-one fuzzy rules with first-order Sugeno FIS, as shown in Figures 5 and 6. The developed structure through the hybrid learning algorithm stipulated inputs-output relationship. The Conventional technique was also constructed based on Hammerstein Wiener using MATLAB (R2013b) command "ident" and "nlhw", as depicted in Figures 7, 8 and 9 respectively. The construction was set to estimate inputs-output relationship using piecewise linear and sigmoid basis function algorithm [17]. The construction was employed the uniformly time-domain inputs-output data to estimate the HW. Each model is trained with combination of hidden layer, as given in Figure 7. The sigmoid basis function used was based on the Neural Network, which consists of input layer, hidden layer and output layer as given by Figure 7.

The following three conditions were controlled the training: (1) maximum epoch (2) minimum error and (3) early stopping condition. The developed models were statistically analyzed using Mean Absolute Percentage Error (MAPE) and Root Mean Square Error (RMSE) as given in equations (5) and (6), to compare the performance of the forecasting techniques and to consider the effect of the magnitude of the actual values and to judge the models. To add more weight in terms of accuracy and perfections to the outperformed model, the prediction criterion in equations (7), (8) and (9) were used. These quantifiers observed the differences between the measured values and the forecasted values from the model. Both are measured in the same units with the actual data. The actual and predicted values of the considered parameters were plotted using Microsoft Excel Package 2016. The SDCCH, TCH Cong. And Intra_HSR were used as the input parameters and one output parameter, HOSR respectively to the construction of the models.

SDCCH and TCH channels are the most affected channels during congestion. These channels are used to locate the exact congestion on the logical channels.

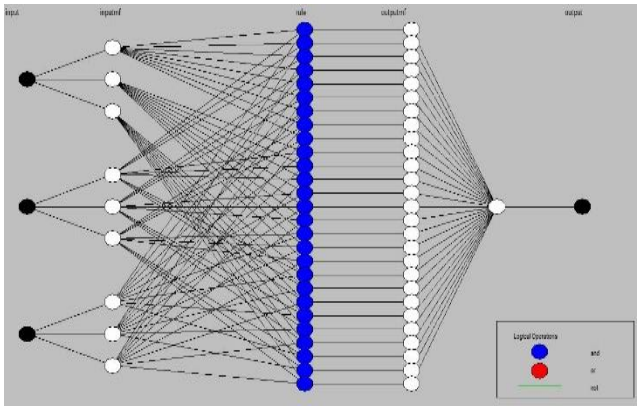

Figure 5. ANFIS trapezoidal mf with first-order Sugeno FIS.

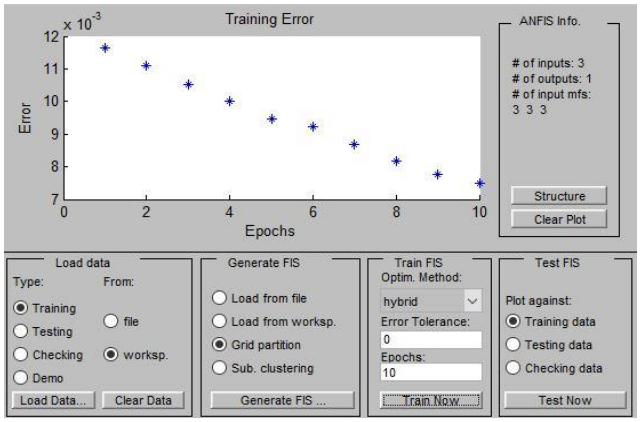

Figure 6. ANFIS Plot with loaded variables

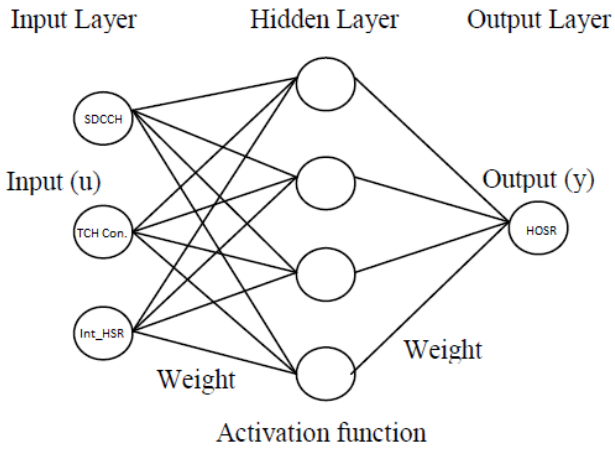

Figure 7. HW nonlinear estimator with adopted Sigmoid activation function structure

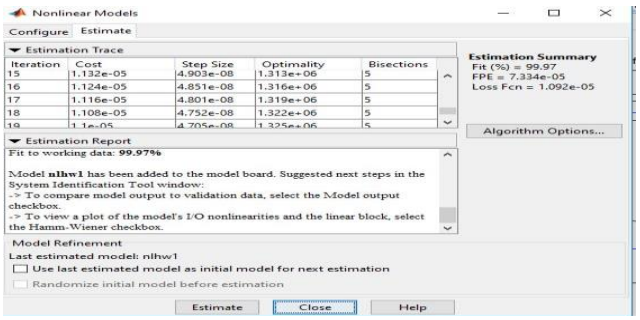

Figure 8. HW workspace with estimated load variables

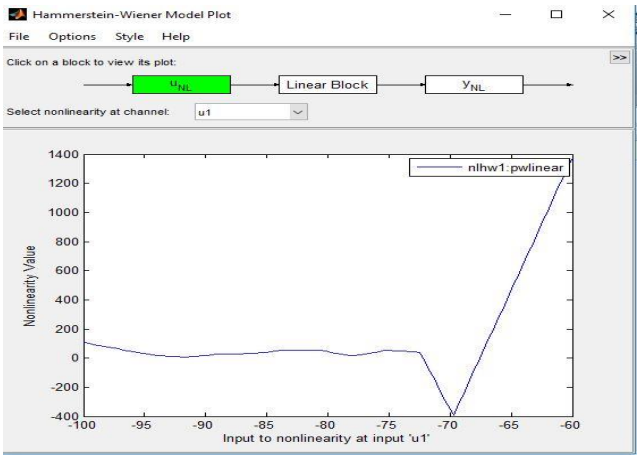

Figure 9. HW Plot of load variables

4 RESULTS AND DISCUSSIONS

The representations in Figures 10 through 13 shows the performances of the trained data, and clearly indicates that conventional method (HW) is superior to intelligent techniques in forecasting HOSR. Tables 1 and 2 are the corresponding prediction tests of the developed models, it is apparent that conventional technique tracked the mapping of HOSR, but there were rare cases where the intelligent technique is superior to the conventional technique that was at S-network data during training.

Table1. The Performance of the Models during the Training Phase

Carriers	Forecasting Techniques	Evaluation Tools	
		MAPE	RMSE
P	ANFIS	0.0014540	0.00001866
	HW	0.0000	0.0000
Q	ANFIS	0.0000002026	0.00002444
	HW	0.0000	0.0000
R	ANFIS	0.0000001656	0.00001924
	HW	0.0000	0.0000
S	ANFIS	0.0000003055	0.00003651
	HW	0.00070208	0.083893

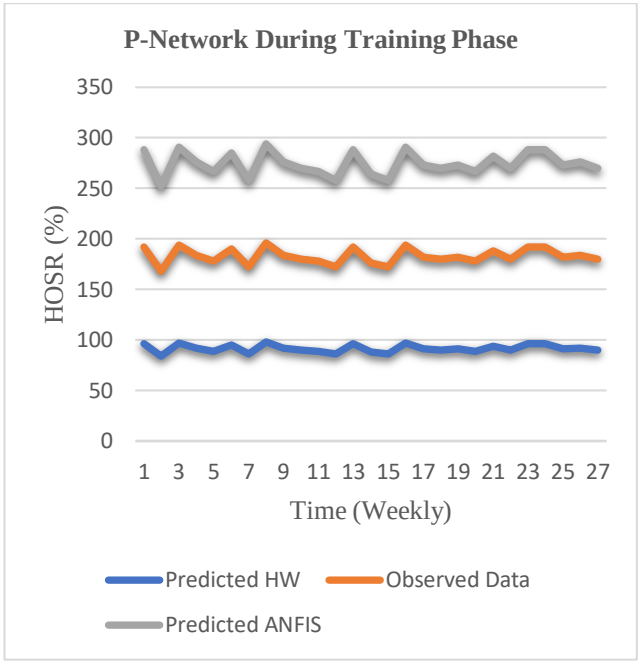

Figure 10. Performance of the P-network data during Training Phase

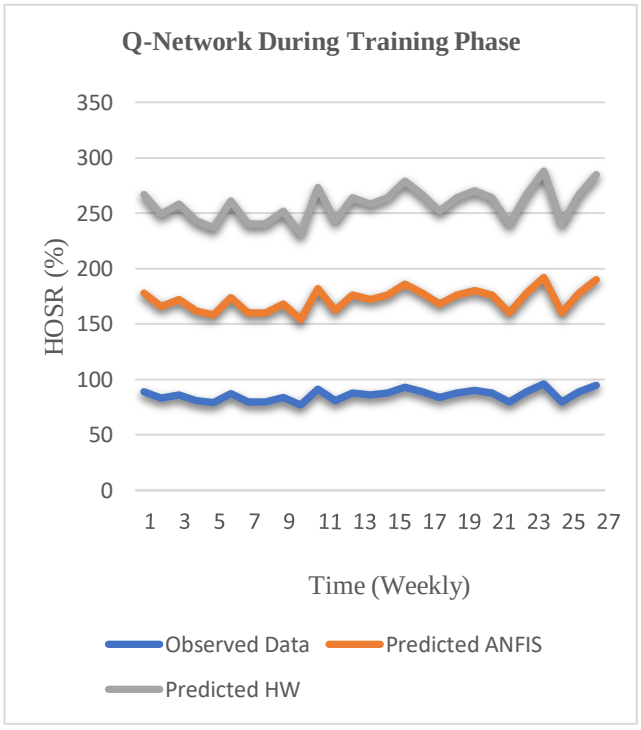

Figure 11. Performance of the Q-network data during Training Phase.

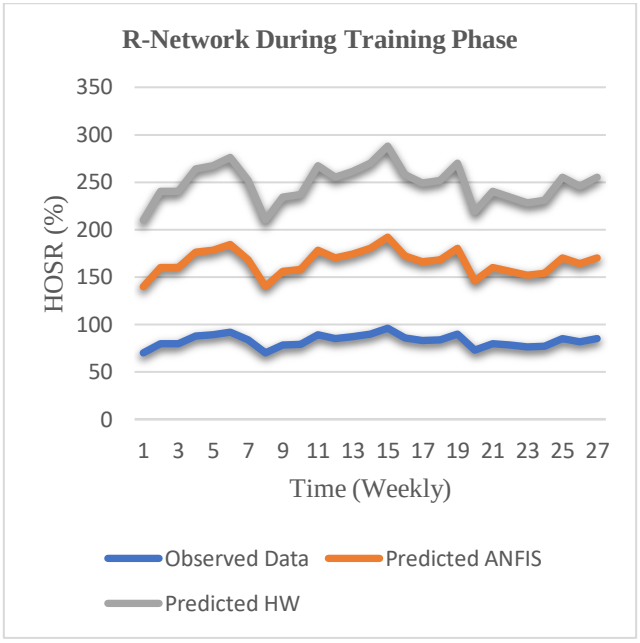

Figure 12. Performance of the R-network data during Training Phase.

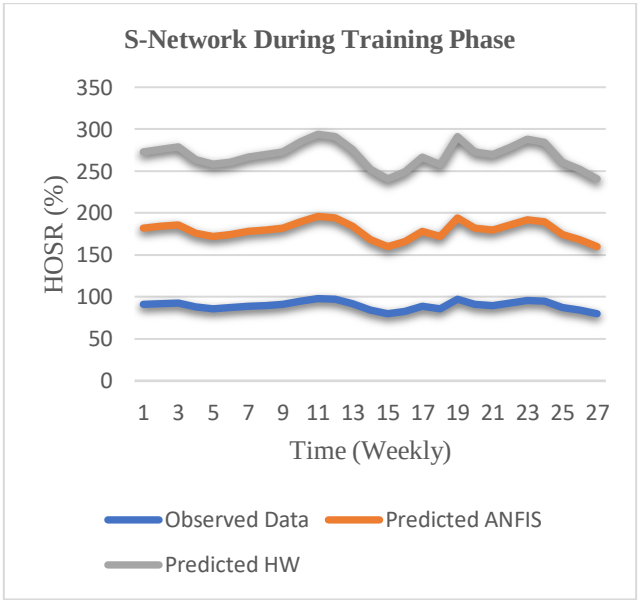

Figure 13. Performance of the S-network data during Training Phase.

4.1 Validation of the Models

The Figures 14 through 17 represent the testing phase, all the predictors were globally and individually significant without any serious violation. The result of the test is tabulated below in Table2. The work in [8] evaluated their developed models using RMSE and achieved the accuracy more around less than 5 % of the considered mobile carrier, but this work achieved RMSE for that considered mobile carriers of 0.00 which is hundred percent perfect, followed by 6 %, 9 % and 45 % respectively of the other carriers

considered in the study. Furthermore, to put more weight on the accuracy and justification and reliability to the developed models, the work adopted MAPE error criteria to build additional confidence to the models, thus it achieved very significant results with less than 10% upon all the four networks, which is acceptable and highly accurate. It is readily identified during test that, ANFIS outperformed HW at the R-network. Henceforth, the evaluation of the outperformed model is also done using goodness of fit criteria, final prediction error and loss function as tabulated in Table3, this will add more weight to the model. These techniques provide valuable tools in forecasting HOSR in the case study area. Finally, the data analysis revealed that the carriers failed at some levels to achieved, Nigeria Communication Commission, NCC threshold of 98 % for HOSR and <= 0.2% for SDCCH Cong. [25].

Table 2. The Performance of the Models during Testing Phase

Carriers	Techniques	Evaluation Tools	
		MAPE	RMSE
P-network	ANFIS	0.3358	50.5677
	HW	0.0000	0.0000
Q-network	ANFIS	0.2834	39.4984
	HW	0.0683	9.4974
R-network	ANFIS	0.0092	6.8271
	HW	0.1810	134.4543
S-network	ANFIS	0.9519	139.6244
	HW	0.0568	45.6185

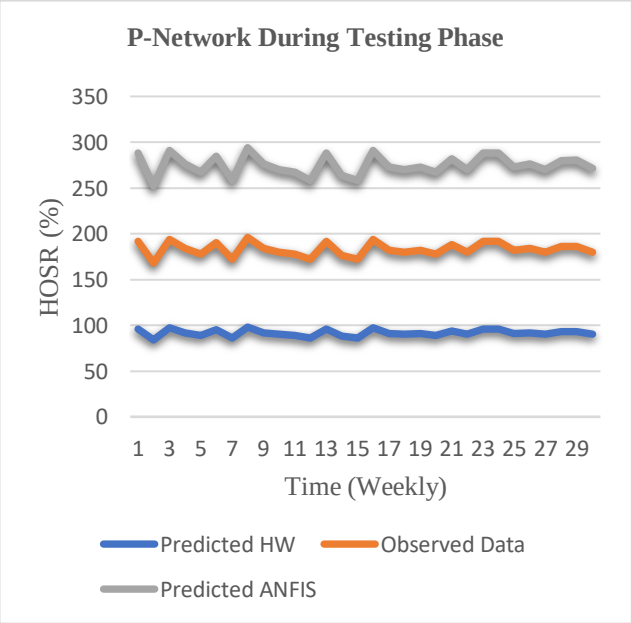

Figure 14. Performance of the P-network data during Testing Phase

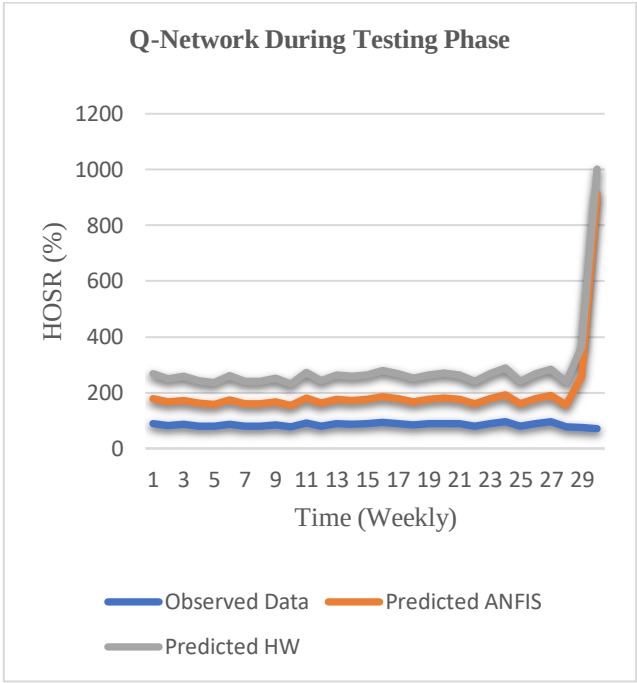

Figure 15. Performance of the Q-network data during Testing Phase.

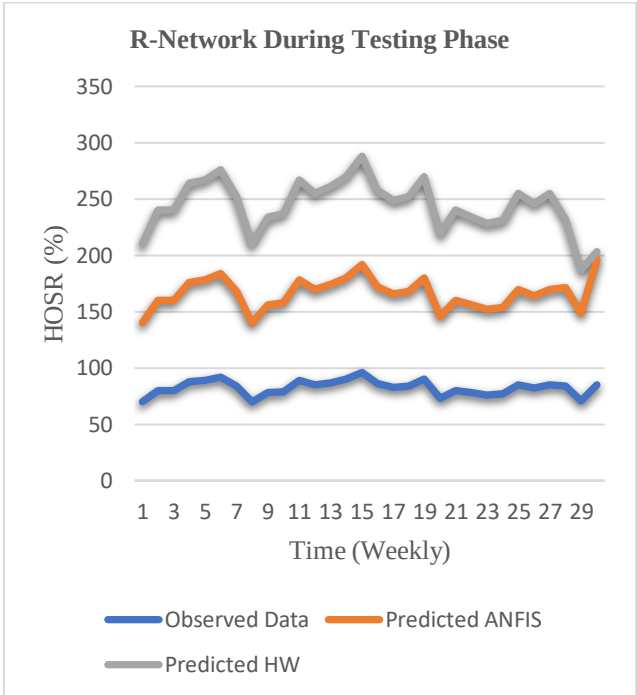

Figure 16. Performance of the R-network data during Testing Phase.

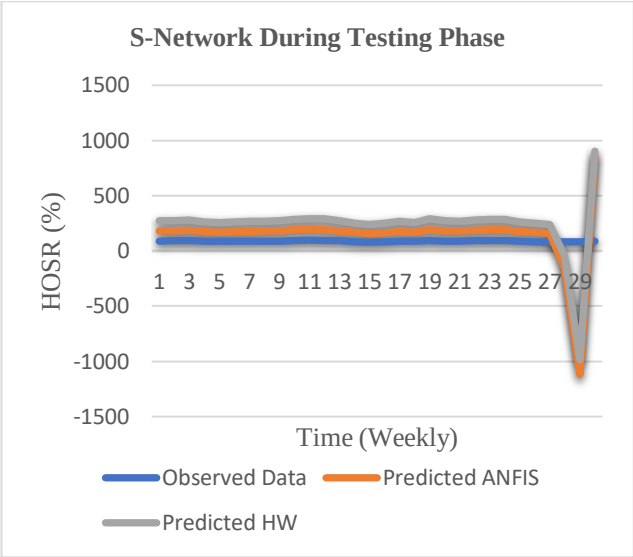

Figure 17. Performance of the S-network data during Testing Phase.

Table 3. Properties of HW Model

Mobile Carriers	Fit (%)	FPE	Loss fcn
P-network	100	3.357×10^{-25}	3.993×10^{-26}
R-network	100	3.672×10^{-26}	4.368×10^{-27}
Q-network	99.97	7.334×10^{-5}	1.092×10^{-5}
S-network	89.34	6.312×10^{-3}	2.012×10^{-4}

5 CONCLUSIONS

The work contributed on the development and construction of precise and reliable techniques for forecasting HOSR on live cellular networks within the case study area, it is applicable not only in forecasting HOSR but also for forecasting other problems. The HOSR is forecasted using HW as conventional technique and ANFIS as intelligent technique. Moreover, the paper performs multiple evaluations of the proposed models, using RMSE and MAPE. The HW and ANFIS techniques lead to major reductions in the ranges of variation of handover operating parameters. Evaluation results reflect that the HW performed better than the ANFIS in predicting the behavior of HOSR. But at R-network and S-Network during testing and training phases the ANFIS outperformed the HW. Hence, the results shows that the improvement using the HW can vary considerably depending on the nature of the carrier's data. Among the two models tested, HW as an outperformed model with piecewise linear and sigmoid network estimators, produced highest percentage of best fit, with the lowest value for FPE and loss function. The work further considers that through numerous combinations of HW properties and appropriate handover value parameters, the best forecasting technique can be determined. The two models could serve as valuable tools in forecasting HOSR, since the RMSE values would be accepted. The paper also provides insight at the rate at which these four mobile carriers are maintaining their handover parameters' setting. Our investigation shows that; the carriers were unable at most levels to meet the threshold metrics of NCC for the SDCCH Cong. and HOSR parameters considered in the paper, this will provide insight to the authorities concerned to take the right decisions. Proper optimization of the above parameters before executing handover process can save time during handover and lead to a generic handover management scheme.

There are still many open issues beckoning further investigations, such as QoS protocols and system traffic etc. that will improve handover in cellular network.

REFERENCES

1. Hadzialic, M. Skrbic, M., Huseinovic, K., Kocan, K., Musovic, I., Hebibovic, J. and Kasumagic, L.: An Approach to Analyze Security of GSM Network. In: Proc. 22nd Telecommunications Forum, Serbia, Belgrade (2014).

2. Galadanci, G. S. M., Abdullahi, S. B. and Usman, A. U.: Modeling the Traffic Load of Selected Key Parameters for GSM Networks in Nigeria, International Journal of Digital Information and Wireless Communications, 9(1), pp. 22-32 (2019).
3. Horvath, G. and Fazekas, P.: End-to-End QoS Signaling Protocol and its Performance Analysis for LTE Networks, Telfor Journal, 6(1), pp. 18-23 (2014).
4. Galadima, A. A.: Analysis and Optimization of Intercell Handover Dynamics in a GSM Network (A Case Study of Airtel Kano, Nigeria, Ph. D. Dissertation, Ahmadu Bello University, Zaria, Kaduna, Nigeria (2014).
5. Jagadesh, B. L., Kullayamma, I. and Naresh, V.: Handover Analysis, IJERA, 1(2), pp. 287-291 (2014).
6. Radev, D., Radeva, S., Kurtev, I. and Stankovski, D.: Priority Handover Schemes in Wireless Networks. In: Proc. of the CSNDSD08 Conference, pp. 433-437, Vienna, Austria (2015).
7. Svoboda, P., Buerger, M. and Rupp, M.: Forecasting of Traffic Load in a Live 3G Packet Switched Core Networks. In: Proc. of the 18th Telecommunications Forum TELFOR 2010, pp. 320-323, Serbia, Belgrade (2010).
8. Galadanci, G. S. M., Abdullahi, S. B.: Performance Analysis of GSM Networks in Kano Metropolis of

Nigeria, American Journal of Engineering Research, 7(5), pp. 69-79 (2018).

9. Nkordeh, N., Olatunbosun, J. O., Bob-Manuel, I. and Oni, O.: Analysis of Mobile Networks Signal Strength for GSM Networks. In: World Congress on Engineering and Computer Science Proc. WCECS Conference, pp. 44-52, San Francisco, U.S.A (2016).
10. Singh, P., Kumar, M. and Das, A.: A Design Approach to Maximize Handover Performance Success Rate and Enhancement of Voice Quality Samples for a GSM Cellular Network. In: 2014 International Conference on Signal Propagation and Computer Technology Proc. ICSPCT Conference, pp. 294-299 (2014).
11. Garba, S., Abdu-Aguye, U. F., Mustapha, A., Yahaya, B. and Salisu, S.: Comparative Analysis of Ann and Anfis in Forecasting GSM Handover Success Rate. In: Proc. of the National Conference on Engineering & Technology for Economic Transformation, pp. 14-17, A.B.U. Zaria-Kaduna, Nigeria (2014).
12. Girma, S. T., Konditt, D. B. O. and Ndungu, K. E. N.: Fuzzy Logic Based Traffic Balancing in a GSM Networks, Journal of Research in Engineering, 1(2), pp. 63-74 (2014).
13. Umoren, I., Asagba, P. O. and Owolabi, O.: Handover Manageability and Performance Modeling in Mobile Communication Networks, Computer, Information System, Development of Information and Allied Research Journal, 5(1), pp. 27-36 (2018).
14. Poole, I.: (2017): Overview of the Essentials of GSM Handover or Handoff. In: A tutorial. [Electronic Medium], Available: http://www.radio-electronics.com [Accessed: 6 October 2018].
15. Galadanci, G. S. M., Abdullahi S. B. and Bature. Z. A.: Forecasting of Traffic Load for 3G Networks Using Conventional Technique. International Journal of New Comp. Architecture and their Applications, 8(4), pp. 206-213 (2018).
16. Lawrence, K. D., Klimber, R. K. and Lawrence, S. M.: Fundamentals of Forecasting using Excel. Forecasting Performance Measurements, Tracking Signals and Randomness Tests 4, 57-61 (2009).
17. Yusoff, Z. M., Muhammad, Z., Rahiman, M. H. F., Tajuddin, M., Adnan, R. and Taib, M. N.: Modeling of Steam Distillation System Using Hammerstein-Wiener Model. In: Proc. of 2011 IEEE 7th International Colloquium on Signal Processing and its Applications, IEEE Press, New York (2011).
18. Patcharaprakiti, N., Kirtikara, K., Monyakul, V., Chenvidhya, D., Sangswang, A. and Saelao, J.: A multi Input Multi Output (MIMO) Hammerstein-Wiener Model Based Predictive Control of Single Phase Grid Connected Inverter, International Journal of Modeling and Optimization, 1(1), pp. 29-36 (2011).
19. Niedzwiecki, M. and Ciolek, M.: Akaike's Final Prediction Error Criterion Revisited. International Conference Paper, DOI:10.1109/TSP.2017.8075977
20. Muhammad, A., Gaya, M. S., Aliyu, R., Abdulkadir, R. A., Umar, I. D., Yusuf, L. A., Ali, M. U. and Khairi. M. T. M.: Forecasting of Global Solar Radiation using ANFIS and ARMAX Techniques. In: IOP Conference Series: Materials Science and Engineering 303 (2018) Proc. ICFMM2017 Conference., pp. 1-3 (2017).
21. Wills, A., Schon, T. B., Ljung, L. and Ninness, B.: Identification of Hammerstein-Wiener Models. In: Proc. of the 18th IFAC World Congress, Milan, Italy (2011).
22. Gershenson, C.: Artificial Neural Networks for Beginners. In: Neural and Evolutionary Computing. Artificial Neural Networks 4, 1–9 (2003).
23. Abdullahi, S. B., Bature, Z. A., Galadanci, G. S. M. and Ali M. H.: Performance Comparison for Voice Services of 3G Networks in Kano Metropolis, American Journal of Engineering Research, 8(4), pp. 218-223 (2019).
24. Pocket Manual.: Ericson W995 and W995a Inc., Reston, USA (2013).
25. Nigerian Communication Commission (NCC), http://www.ncc.gov.ng/technology/standards/qos

International Journal of New Computer Architectures and their Applications (IJNCAA) 9(1): 11-18
The Society of Digital Information and Wireless Communications, 2019 ISSN 2220-9085 (Online); ISSN 2412-3587 (Print)

Further Development of Boost Chopper for Power Conditioners
- Pursuit of ideal PCS for photovoltaic power generations -

Keiju Matsui 1,2, Eiji Oishi 1, Masayoshi Umeno 1
Mikio Yasubayashi 2, Yuuichi Hirate 2, Sudip Adhikari 2, Masaru Hasegawa 2

1; Minna-denryoku, Inc., Setagaya Monozukuri Gakko 210, Setagaya 154-0001, Japan
2; Chubu University Kasugai, Japan

ABSTRACT
Under an environment of praise for renewable energy, photovoltaic power generations (PVG) have been applied generally and spread broadly. Various power conditioning systems (PCS) used in those have been also studied by many researchers. In addition to usual utilization, such PVG is often considered for the time of disaster. Usually such PVG systems having limited power are almost installed in limited area such as on top of the roof of the building. Some medical institutions have fairly desire to install such PVG since they must avoid the medical service interruption. The generating power in such case is fairly limited, so the system construction should balance the reduced power. Thus, it is necessary to improve the construction toward simple one. In usual PCS, power is converted by two stages, that is boost converter and normal inverter. In first stage, the dc power is adjusted to appropriate voltage level. The conversion methods are considered in many strategies. In this paper, in order to pursue an ideal one, simple and concise power converter, especially novel boost chopper is proposed. Considering fair reduced power and narrow space of installation, the system constructions should be compact. The circuit that gratifies their operating characteristic is presented and analytically discussed about circuit construction as a novel boost converter. The circuit operation is confirmed by using the circuit software and a few experiments.

KEYWORDS: Power Conditioners, PCS, Solar cell, Boost chopper, Photovoltaic power generation, PVG , Power delivery flowchart

1 INTRODUCTION

In modern medical care, the development of the structural function in the operating room is remarkable. The endoscopic surgery including surgical robot and the catheter intervention has been applied, so that such remarkable operating technics have been developed with robotic operating room and hybrid operating room. For almost electrical equipment using in such medical facilities, even instantaneous interruption could not be permitted.

In general, by means of large capacity uninterruptible power supply installed by generator and batteries, the medical service may be kept and provided. In such system, however, the installed scale becomes large accompanied by extremely high cost.

The power conditioners-PCS including boost converter have been presented in various systems so far [1,2]. However, it is necessary to reduce the cost even more. It is said that the system is approaching to an ideal one with respect to efficiency and construction strategy, but that cost would prevent widespread. In such discussions, there are many subjects to be resolved to utilize the PV power effectively. Even more, various safeguard equipment required according to regulations make the cost increase. Thus, it is required to obtain even lower cost PCS. In fair reduced power PCS as mentioned, the equipment are installed in limited facilities. In such case of reduced generating power, that is, in such PV power generation systems, there are so many subjects to be resolved [3].

The authors have been pursuing an ideal PCS in a series of the small power PV system [4,5]. In this paper, some simple PCS systems, especially the boost chopper is presented and discussed toward simple construction with some experiments. The whole result is analytically performed and discussed.

2 DISCUSSIONS ON VARIOUS UNIQUE BOOST CHOPPERS

2.1 Prologue of Boost Chopper

In the early years, the usual interconnected PCS is provided through the bulky transformer which cuts off the dc component from the output power system. As shown in Fig.1 of the conventional system, the transformer is necessary. However, such construction prevents the low cost and size reduction. In recent methods, by means of high performance and high reliability, dc power can be

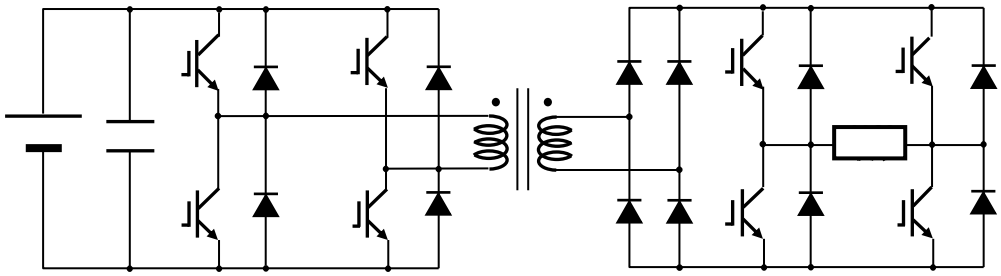

Figure 1. General PCS in early times.

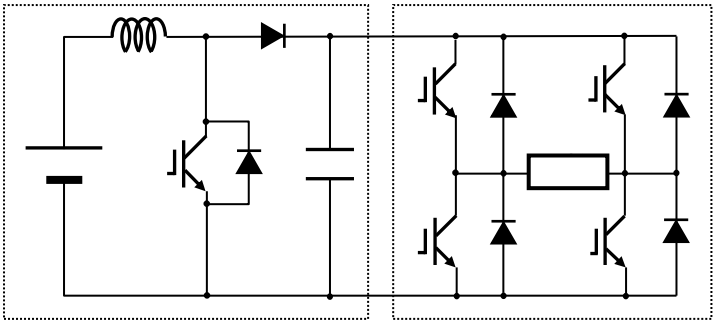

Figure 2. General PCS in recent years.

easily removed as shown in Fig.2. Just mentioned PCS without transformer is superior with respect to low cost, downsizing and lightening in weight. However, with respect to the conversion efficiency even in such PCS using transformer-less converter, there is some room to improve that efficiency of conversion by means of varying combination of circuit component. In this section, some original circuit configurations are presented, which are compared with some conventional schemes. Fig.3 shows various converters which includes original ones in Fig.3(b), (c) and (f), those are proposed by one of the authors [5,6].

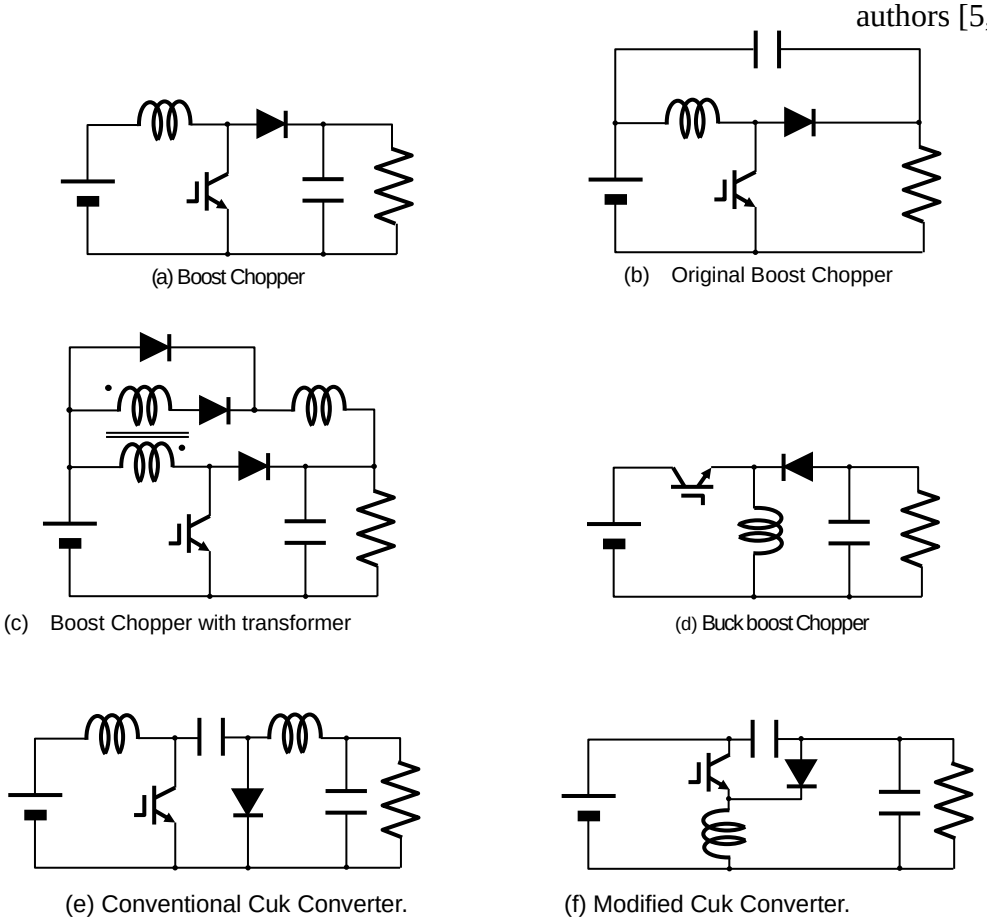

Figure 3. Various DC-DC Converters.

2.2 Operation of Conventional Boost Chopper

The boost chopper is to boost the input dc voltage, which is often used for general power conditioners-PCS under discussion about photovoltaic power generation. As the output voltage becomes higher than the input solar panel voltage, so the diode D prevents the reverse current flow. The output capacitor voltage E_o is smooth and constant due to the large capacitance C. The equivalent circuit at switch S turning on or off are represented by Fig.4(a) and (b), respectively. Analytical operation can be obtained as follows;

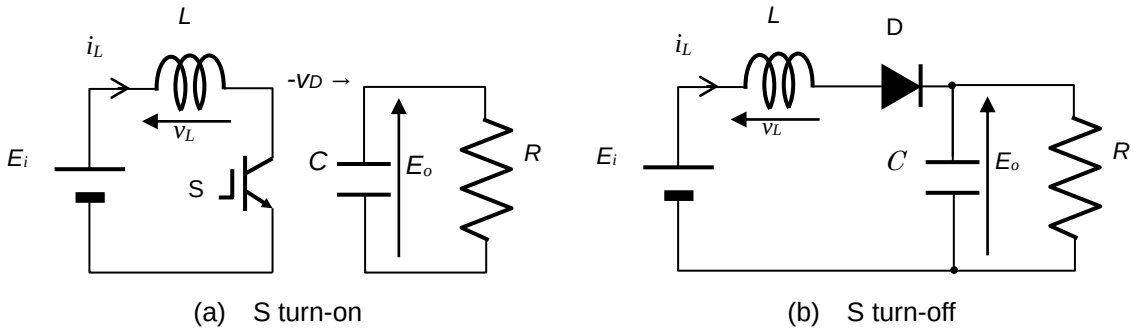

Figure 4. Operating Circuits of Usual Boost Chopper.

When switch S is turned on, the diode D in Fig.4(a) is reverse-biased. The input voltage is applied across the inductor L as shown in the figure. In the boost chopper operating in the current continuous mode, inductor voltage and its current can be obtained as following expressions;

$$v_L = L\frac{di_L}{dt} = E_i \qquad (1)$$

$$i_L = \frac{E_i}{L}t + i_L(\mathrm{O}) \qquad (2)$$

At $t = T_{\mathrm{off}}$ when S is turned off, the reversed voltage across L is added to the supply voltage and the current is flowing into the load. The stored energy in the inductor is delivered towards the load. The relationship is given by

$$v_L = L\frac{di_L}{dt} = E_i - E_o \qquad (3)$$

Because of $E_i \leq E_o$,

$$i_L = \frac{E_i - E_o}{L}(\mathrm{t} - T_{\mathrm{on}}) + i_L(T_{\mathrm{on}}) \qquad (4)$$

From these equations,

$$E_o = \frac{1}{1-d}E_i \qquad (5)$$

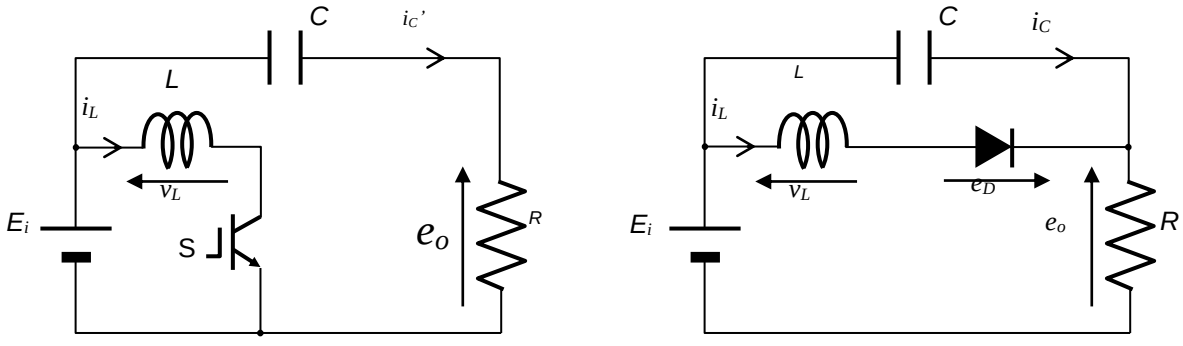

Figure 5. Operation Circuits of Original Boost Chopper.

3 PROPOSAL OF NOVEL BOOST CHOPPER

Fig.5 shows the original boost chopper. As compared with the circuit in Fig.4, instead of the

smoothing capacitor, that capacitor connection is moved to the terminals between input supply and output load as shown. The circuit operation is a little different. However, the principle of the intrinsic operation is the same compared to just mentioned mechanism. The most important difference is to make possible to reduce the smoothing capacitor voltage.

4 POWER FLOWCHART OF ORIGINAL BOOST CHOPPER

The power transmission flowchart for original one is presented in Fig.7. In order to compare the operational mechanism with usual one, the power delivery flow chart for conventional boost chopper is described in Fig.6 at first. In the figure, d is on-duty cycle and d' is off- duty one. I_i is input current and I_o is output current. As S is turned on with duty cycle d, the power $E_iI_i\,d$ and $E_oI_o\,d$ are delivered from E_i to L and C to E_o, respectively. When S is turned off with off-duty cycle d', the power E_oI_od' and $(E_o\text{-}E_i)I_id'$ are delivered from E_i to E_o and L to C, respectively The power delivered process becomes different, and efficiency may be deteriorated accordingly. In comparing between Fig.6 and Fig.7, the difference of delivery mechanism can be confirmed.

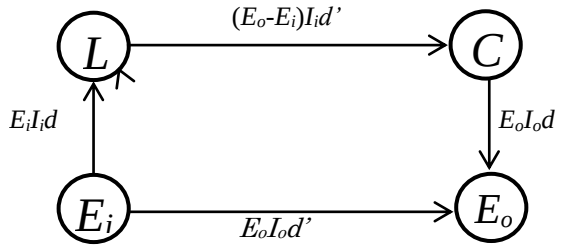

Figure 6. Power Flowchart of Conventional Boost Chopper.

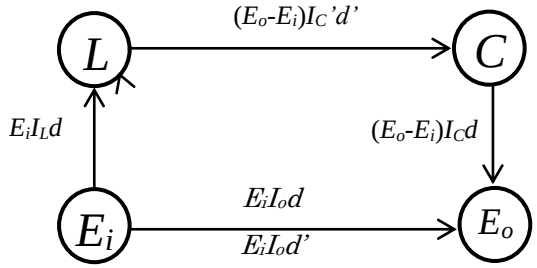

Figure7. Power Flowchart of Original Boost Chopper.

In Fig.7, when S is turned on in duty cycle d, the power $E_iI_L\,d$ and $(E_o\text{-}E_i)I_Cd$ are delivered from E_i to L and C to E_o, respectively. At the same time, the power is delivered from E_i to E_o as E_iI_od.

During period of d, C is discharged as shown in Fig.5.(a) as I_C'. When S is turned off, C is charged as I_C. The relationship of capacitor discharge current I_C and charge current I_C' can be given by following equations;

During charge period of d', the capacitor is charged by $I_C'\times d'$. On the other hand, during discharge period, C is discharged to $I_C\times d$ by inductor L. During discharge period, $I_C = I_O$.

Total electric charge q' for d' is

$$q' = I_C'd' \qquad (6).$$

For discharge period when S is turned on, electric discharge q is

$$q = I_C\,d = I_O\,d \qquad (7).$$

As $q = q'$, relationship of

$$I_C'd' = I_O\,d \qquad (8)$$

can be obtained as

$$I_C' = I_O\times d'. \qquad (9)$$

When S is turned off with off-duty cycle d', the power E_oI_od' and $(E_o\text{-}Ei)I_id'$ are delivered from E_i to E_o and L to C, respectively In comparison of these figures, the following description will be confirmed. For example, direct transmission from power supply to the load,

$$E_oI_od' = E_iI_id' = E_iI_od + E_iI_od' = E_iI_o \qquad (10)$$

Since $I_id' = I_o$ (11)

this equation is confirmed by following establishment.

The significant difference is the input current flowing situation. For the usual boost chopper, the input current value is constant because of large value of inductor. On the other hand, for the proposed boost chopper, during S turned on period, the current is flowing towards load. As a result, The input current is

$$I_i = I_o + I_L \qquad (12)$$

During S turning off

$$I_i = I_L - I_C \qquad (13)$$

From these equation, the average input current,

$$I_{avi} = (I_L\,d + I_C\,d') \qquad (14)$$

The withstanding capacitor voltage is given as shown.

For conventional one,

$$V_{Cwith} = E_O \qquad (15),$$

For the original one,

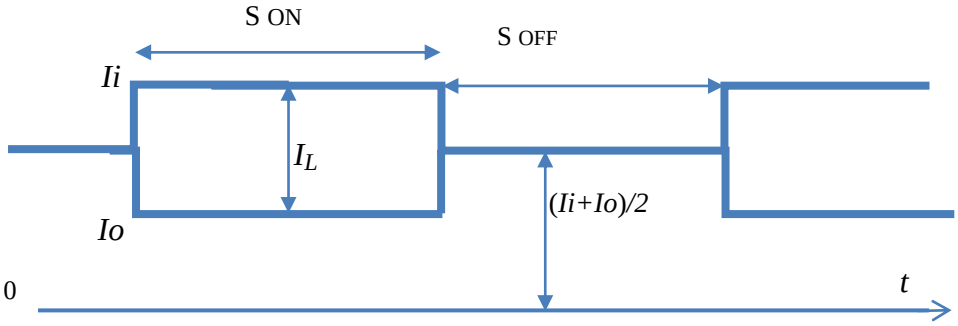

Figure 8. Input and Output Current.

$$V_{Cwith} = E_O \times d \quad (16)$$

It is said that the capacitor price is increasing according to the applied voltage. So, this characteristic may be favorable construction.

5 EXPERIMENTS

Fig.9 shows the experimental results for various choppers to boost the input dc voltage. The results for original boost chopper is favorable one, whose results is almost the same compared to conventional boost chopper even by reduced voltage of capacitor. The results for converter having the transformer is showing the next favorable result. If on the design procedure, the transformer is taken for larger size, the efficiency will be given for the best one. With respect to the Cuk ones, the conversion efficiency is going to a little worse. The reason is due to the many stage for power conversion. Finally, we can say that the buck boost type is the worst result. The reason is there is no direct power transmittal operation.

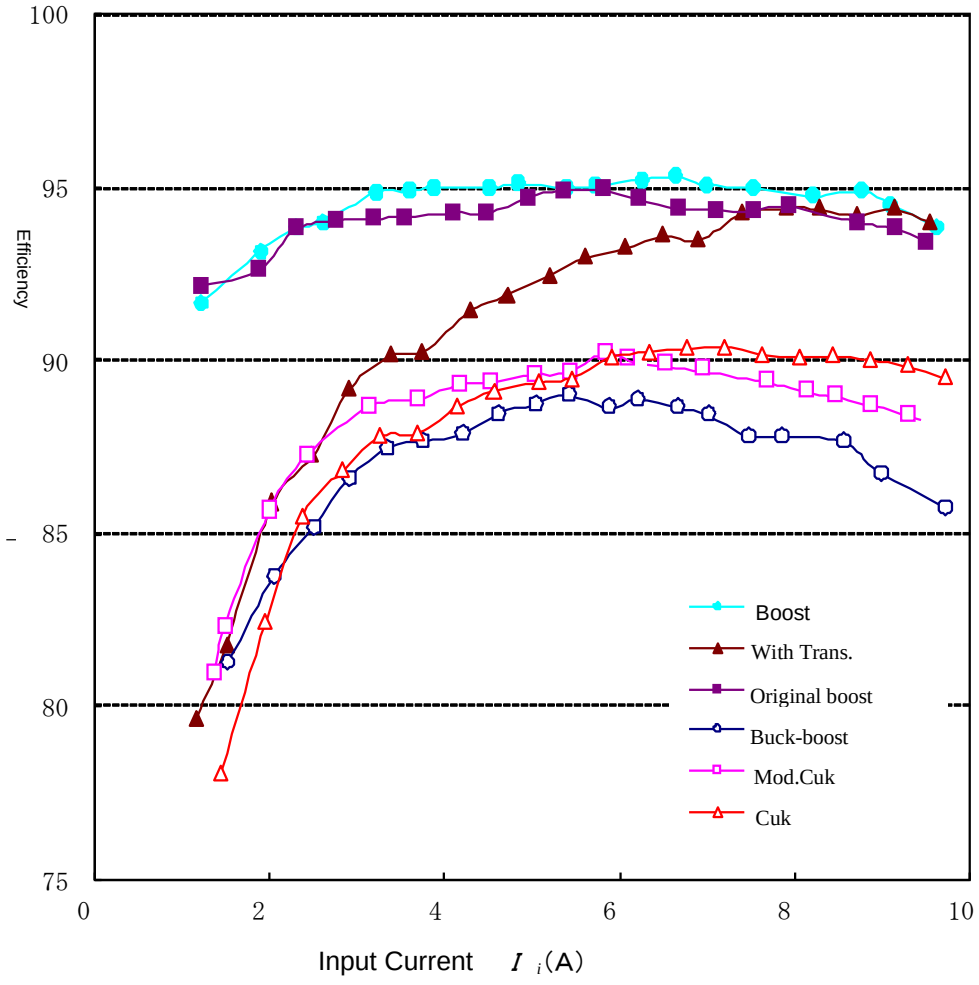

Figure 9. Experimental Results for Various Boost Choppers.

That is, once the whole power is stored in the inductor, after that, the whole power is delivered to the load. That operation needs the bulky inductor and creates large energy loss.

6 CONCLUSIONS

A few proposed circuit strategies are proposed and confirmed in theoretical and experimental procedures. Various ideas are applied to power conditioners for the photovoltaic power generation systems, whose idea is obtained from the usual PCS, which is constructed by chopper and inverter circuit. So far, various PCS have been devised and applied by many researchers. In this paper, about boost chopper of first stage, a few circuit strategies having novel ideas are presented and discussed. With respect to trans-less combination, a few boost chopper is treated and analyzed satisfactorily. In such a case, the high cost and high voltage smoothing capacitor could be avoided. In addition, the rest of the other choppers can also present its superior feature.

ACKNOWLEDGEMENTS

This research is mostly supported by a grant of Research Institute for Life and Health Sciences of Chubu University - Short Term Research Project). We would like to express our appreciation to who it may concern about this project.

REFERENCES

1. C.-M. Wang; “A novel single stage full bridge buck-boost inverter”, *IEEE Trans. on Power Electronics*, vol.19, pp.150-159, 2004

2. C.-M. Wang; “A novel single stage series resonant buck-boost inverter”, *IEEE Trans. on Industrial Electronics*, vol.52, pp. 1019-1108, 2005

3. Keiju Matsui, Eiji Oishi, Yasutaka Kawata, MikioYasubayashi, Masayoshi Umeno, Hideo Uchida, Masaru Hasegawa, “Pursuit for Simple Power Conditioner and System Construction of Photovoltaic Power Generation as Veranda Solar”, Proceedings of the 3rd International Conference on Industrial Application Engineering, pp.531-536, 2015-3
4. S.Miyake, K.Torikai, S.Naruse, S.Hirose, I.Yamamoto and K.Matsui, “Improvements of Utility-Interactive Photovoltaic Power Conditioning Systems for Domestic Applications”, 」 ,IEEE Industria1 Electronics Conference, IECON 2000, Conference Proceedings, pp.989-995 （2000-10）
5. Masayuki Matsuo, Keiju Matsui, Isamu Yamamoto and Fukashi Ueda, “ A Comparison of Various DC-DC Converters and Their Application to Power Factor Correction”, IEEE Industrial Electronics Conference, IECON 2000, Conference Proceedings, pp.1007-1013 2000-10
6. Fang Zheng Peng:“Z-Source Inverter”, IEEE Transactions on Industry Applications, Vol. 39, No. 2, pp.504-510, March/April 2003
7. Keiju Matsui, Eiji Oishi, Yasutaka Kawata, Mikio Yasubayashi, Masayoshi Umeno, Hideo Uchida, Masaru Hasegawa: “Proposal of Boost-Inverter having Voltage Double Capability”, The Proceedings of ICEMS-2016, DS1G-2-1, 2016-11
8. Keiju Matsui, Eiji Oishi, Yasutaka Kawata, Mikio Yasubayashi, Masayoshi Umeno, ,Masaru Hasegawa: “Pursuit of Simple PCS for Photovoltaic Power Generation – Optimum Waveforms”, IEEE-Intelec 2015, pp.915-920, 2015-10
9. Hiroshi Unno, Masanori Hayashi,Yoshiaki Matsuda, “High Efficiency Low Output Voltage DC/DC Power Supply”, IEICE, 2000-58, pp.41- 48, 2001-2
10. R.O.Caceres and Barbi, “A boost DC-AC converter; analysis, design and experimentation, “ *Trans. On Power Electronics*, vol.14, pp.134-141, 1999
11. Keiju Matsui,Eiji Oishi, Mikio Yasubayashi, Yuuichi Hirate, Sudip Adhikari, Masaru Hasegawa、” Circuit Analyses and Considerations on Advanced Inverters Constructed by Minimum Circuit Components — Pursuit for concise PCS of photovoltaic power generations — ” . International Journal of New Computer Architectures and their Applications (JINCAA), Vol.8, No.4, pp.179-185, Dec. 2018

APPENDIX

A. Buck Boost Chopper

This converter is presented in Fig.3(d) as the most well-known converter. The obtained characteristic is the worst one. The reason is explained with using original power flowchart as following description;

In this converter in Fig.3(d), in order to prevent direct short current from the input to output load, reverse direction diode is connected. As the switch S is turned on, input inductor current i_L is given by

$$i_L = -\frac{E_o}{L}(t - T_{\text{on}}) + i_L(T_{\text{on}}) \quad \text{(A1)}$$

When S is turned off.

$$v_L = L\frac{di_L}{dt} = E_o \quad \text{(A2)}$$

The output voltage E_o can be expressed shown as

$$E_o = \frac{d}{1-d}E_i \quad \text{(A3)}$$

When duty cycle can be given from 0 to infinity, the obtained voltage region of buck boost chopper can be also given from 0 to infinity. For example, as above experimental result, in order to obtain double output voltage, 200 V compared to the input voltage, 100 V, d = 2/3 is given as duty cycle. As explained, if adequate value of duty cycle is given as setting value, the boosted output voltage can be obtained as desired value. According to mentioned procedure, the power flowchart of buck boost chopper is presented in Fig.A. In the figure, as it can be seen, all energy of delivering is temporarily stored in the inductor L, then those energy is delivered to each component and the load. From this reason of the operation, efficiency becomes deteriorated. As shown in the experimental results, this deterioration due to such operation mechanism is described clearly.

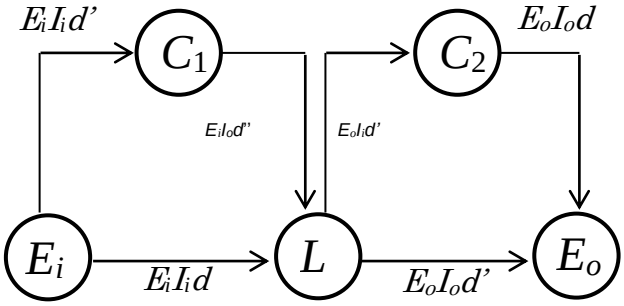

Figure A. Power Flowchart of Buck boost Chopper.

B. Boost Converter Having Auxiliary Transformer

Fig.B shows the original boost converter having the auxiliary transformer. The auxiliary transformer is added in the circuit configuration. In the figure, the primary winding inductor is L_1, and the secondary winding is given by L_2. In the auxiliary transformer circuit, another inductor is connected as L_3. Let the turn ratio of winding of L_1 and L_2 be N_1 and N_2, respectively. In the transformer, if the relationship of turn ratio is, $N_1 : N_2 = 1 : 2$, the output voltage of L_2 becomes double with respect to that of L_1. The operation circuits for turn-on and turn-off are represented in Figs.B(a) and B(b), respectively. One cycle operation is obtained as follows; Firstly, in Fig.B(a), when S is turned on, the supply voltage is applied across the inductor L_1. As a result, the output L_2 voltage is generated as double voltage in this case. In the load, the current i_2 is flowing whose energy is stored into L_3. On the other hand, the operation circuit for S turned off is shown in Figs.B(b). During this period, the analogous operation compared to usual boost chopper is executed. At the same time, the stored energy of L_3 in the last period is delivered to the load. The operation circuits for turn-on and turn-off are represented in Figs.B(a) and B(b), respectively. Thus, we can say that both during turn-on and turn-off period, the output current i_4 is kept flowing in this boost converter having auxiliary transformer. As the voltage polarity of primary and secondary sides of transformer is opposite direction, the

direction of v_{L1} andv_{L2} is shown in opposite ones each other.

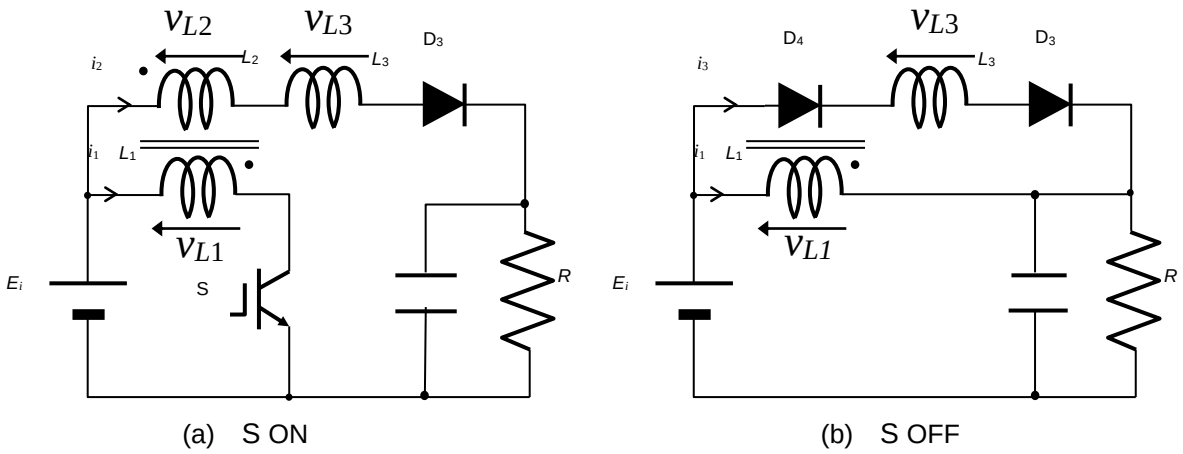

Figure B. Boost Chopper Having Auxiliary Transformer.

International Journal of New Computer Architectures and their Applications (IJNCAA) 9(1): 19-24
The Society of Digital Information and Wireless Communications, 2019 ISSN 2220-9085 (Online); ISSN 2412-3587 (Print)

A REVIEW ON SPIDER ROBOTIC SYSTEM

Mehmet Çavaş 1 and Muhammad Baballe Ahmad 2
[1,2](Mechatronics engineering, Firat University Elazig, Turkey)
Corresponding author: Muhammad Baballe Ahmad
E-mail: ahmadbaballe@yahoo.com

ABSTRACT
The spider robot is a device used in monitoring surroundings wirelessly. This review work will assist in solving the weak adaptive ability of ordinary existing robots. The spider robots function without interfacing, it can easily adapt to the new situation or obstacles due to its legs of locomotion on like the ordinary two legs robots. A spider robotic system will help in monitoring of toxic or nuclear environments and moving in an environment that ordinary robots cannot do like; climbing of walls, rough surfaces, trace and locating of missing items. The user of this spider robotic system poses a perfect resolution to such problems, eradicating the demand for humankind to access such places and regularly providing information on the state of such environment that would not otherwise be available for humanity.

KEYWORDS: , Microcontroller, National Instrument, Sensor, Spider robot, Toxic enviroment

1. INTRODUCTION

In the second half of the 20th century, humankind obtained the rewards of several far-reaching scientific discoveries that normally took place in the first half, amongst which was the control of the nuclear chain reaction for generating electricity [1]. Due to its high energy density and thus relatively small requirement for fuel, nuclear power has been exploited. In addition, it has authorized enhancements in the toughness of materials that were used in the nuclear facilities, and this has led to prolonged achievements and improved safety margins. As results to this, improvements in engineering and materials science have been enforced to a wide of nuclear-connected projects, which stretch from the framework of a rector and additional buildings through to the processes by which they are disbanded [2]. For instance, static and monorail-type teleoperated machines have been in usage since the beginning of nuclear energy to handlebar activities carefully in zones of life-threatening radiation disclosure and to accomplish polluted constituents (Hamel and Martin, 1983; Wehe et al., 1989); while a number of mobile samples were existing during the1960s (Clark,1961; Huffman,1962)[3]. With the help of microprocessor technology booming in the mid-70s, researchers proposed different but possible robotic designs that could replace human on a wider range of work jobs in radiation surroundings; this may include inspection, maintenance, and repair in such environments [4]. Also at the same time, civil nuclear power plants were established in Europe and North America on a scale never repeated since, and hence it made sense to design and build embracing robotic technology for these purposes [5]. In 1979, the necessity for progressive robotic proficiency became a vital because of the reactor disintegration that took place in Unit 2 at Three Mile Island meant that several jobs had to been commenced remotely, accompanying the use of long-handled tools and what were then novel vision systems [6]. At this time the first ever radiation inspection robot, for this objective, used in the basement of the unit four years later regarded as a landmark in the nuclear industry [7]. About seven years after the Three Mile Island accident, the tragic accident that took place in Chernobyl caused in a policy to entomb the damaged plant in sand and clay to restraint the magnitude of the ongoing radioactive secretions, and reformed the interest in the idea of using mobile robots in place of individuals for nuclear accident response applications [8]. The technological enhancements over the next two eras have driven the design and execution of highly refined systems, with robotics gaining more and more popularity in majority commercial fields, such as entertainment, transport, and medicine [9]. Most of the robots that we are familiar with uses wheels for their movement [10]. They can accomplish high speed and relatively small control complication but, even with complex suspension systems, they present many limitations in irregular and rough environments (e.g., hazardous environments and uneven ground) with the help of legged spider robotic systems, and most of these difficulties were

overcome, thanks to its litheness and ground adaptation [11]. Definitely, the opportunity to choose between different available solutions and to adapt and control the position of the center of mass of the system allows dodging slippage and downturns due to environment irregularities [12]. The costs that have to be paid are the lower speed of locomotion and higher complexity of the controller with respect to wheeled systems. Also, due to the fact that the legs are self-reliant controlled, legged systems have a large number of degrees of freedom (DOF) to be coordinated in order to control the position, balance the forces (e.g., load, external forces) and consume as little energy as possible [13]. Since the task of finding an optimal force allocation was made in real time, fast processes and control functions have to be used, as likewise when a body force command solution is not reachable and a new plan has to be formulated [15]. Spider legged robots have a body and a number of articulated legs that start from it. Each of these kinematic chains can also be view as a manipulator that acts like a limb and adds to the overall position and equilibrium of the spider robot structure. In order to estimate and produce an operative legged spider robot, the awareness is to draw motivation from nature [16]. In nature, different legged systems can be able to walk and climb different surfaces with low energetic consumption and high autonomy was been found. Indeed, safe attachment to and easy detachment from smooth substrates is a major feature of a diverse range of animal species. Attachment without using fluids, so-called dry adhesion, were exploit by geckos and Evarcha arcuata spiders by means of fibrillar elements [17]. The adhesion force seems to be related to the approaching angle between the attaching elements and the surface: the maximum adhesion condition reached when the angle is around 30°; a sliding condition occurs when the angle is smaller, and detachment occurs when the angle is bigger [18,19]. Currently, there are some certain conditions in which human beings are incapable to complete a certain mission in this real life, such mission include locating a lost object or items or finding a missing individual in a jungle for more than a day and also discovering a pothole with lack of oxygen and also working in a toxic environments [20]. In order to achieve such problematic tasks, the human being will have to rely on mobile robots [21]. Scientists nowadays show emphasis on the new design of a self-adaptive robotic system, which includes path tracing [22]. In the year 2011, Pratihar, Roy and Singh estimated the optimal bases forces and joint torques in the real-time process for the monitoring of the six-legged robot [23]. This researcher concentrated on finding the best point in the circulations of the bases forces and values of the joint torques of the six-legged robot online [24]. The minimization of the standard of the joint torques and the base forces was been simulated in their study. Roy conducted another research in the same year with Pratihar discovered that unlike duty features will lead to many energy intakes. This duties factors can also differ among 2/3 and 1/3 whereas energy intake will change in the range of 2% and 35% [25]. In the subsequent year, both Pratihar and Roy conduct another research on the legged robot and simulated the technique of attaining extreme steadiness with the minimum energy intake steps. Menon, Henry, and Boscariol, in the year 2013, examined on resolving the unsuitable relocation of forces in the reloading of the legs in the climbing robots which may likely lead to the irreversible dispassion of the spider robots from its upright facades [26]. This researchers finally concluded that it is likely to save 35% of the whole charges of this spider robot if the designed step is well-organized. In this study work, the National Instrument (NI) protocol was been nominated to relate with the suggested well-designed robotic supervisor for interfacing and processor [27]. The suggested smart system gathers data about the environments particularly in available areas and aids the robot to choose the finest route course to be taken. The National Instrument (NI) implanted field programmable gate array (FPGA) board has been selected to merge with spider robot for the tenacity of high enactment adeptness as well as being user-friendly and compatibility. The categorization of leg actions is predefined in this study for persistent walking. With the help and combination of several sensors on its frame construction, this suggested six-legged flexible smart spider robot is fit to be employed in ambiguous environments [27].

Figure 1: Spider robot

2. Materials and Method

2.1 The method used to produce a spider robot

The recommended spider robotic system is divided into (3) three subsystems, which may likely include; the body structure of the spider robot, its sensor, and control algorithm. The configuration of the spider robot is made of aluminum; this is because of the strength of aluminum in resisting the tensile and pressure stress on its exterior. Stalemate bolts were used to protect the position of the National Instrument (NI) board on the framework. Several sensors are applied in the spider robotic body [19-22]. The body of this spider robot must be tough enough to support the heaviness of the National Instrument (NI) board in vigorous circumstances. Henceforward, the consideration that has been taken during the blueprint stage of the spider robot of the main body of the robot this include compression and tensile stress alongside the axis of the movement of this moving parts of the spider robot caused by the burden carried. The six-leg pairs of the spider robot will be attached on a frame of the spider at certain angles that will enable it to maintain the stability and the whole spider robot will be controlled remotely. In order to help keep this spider design steady to avoid it from losing balance or sloping over you will need to assemble the leg pairs and the structure at an angle from the conservative straight ahead. Because the pairs of legs will be pointing at different angles than straight ahead then their directional vectors do not point in the direction of movement, rather at the exact angle from the 90-degree line down the middle of design signifies straight ahead from an outside perspective. This result in two vector quantities chain together and gives magnitude and force in precisely the same path. A servo bracket is fixed to the joint of the legs, each of these different legs of the spider robot has (3) three degree of freedom (DOF). Among the degree of freedom (DOF), one of this degree of freedom is alongside the z-axis and also function as the shoulder and the turning of this shoulder will serve as a controller to the other two joints. This shoulder will be master and the location of it will vigor the other two to take their spot. The National Instrument (NI) board helps in the control of the movement of these joints. Each of these joints uses a servo bracket to a joint to each other. The whole project of the spider robotic system is carried out using feedback loop graphic NI LabVIEW interfacing with an insolent controller and also with the help of the company of smoke sensor, LM35 temperature sensor, and GH-311 ultrasonic sensor. This GH311 ultrasonic sensor produces an exact and non-contact space dimension. When there is a difficulty as far as like 31cm away from this spider robot, with the help of the GH311 sensor it will transfer a high indication to the National Instrument (NI) board to specify the position of the problem and implement the suitable moving algorithm to dodge such hitch. The GH-312 sensor was applied in the spider robot construction to identify hydrogen, smoke, alcohol, liquefied gas, butane, and propane.

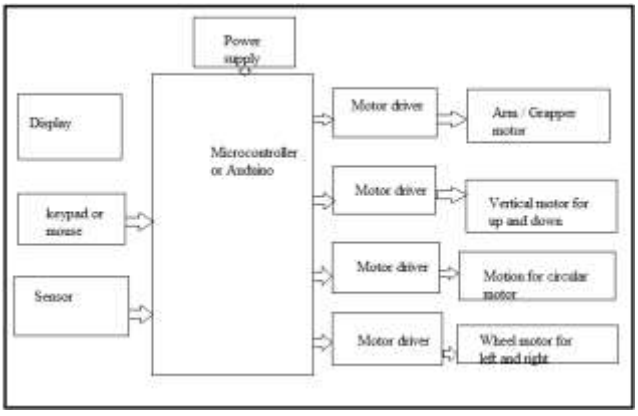

Figure 2: Block diagram of the spider robots

2.2. The principle operation of the spider robot

With the help of the Arduino receiver or microcontroller, it takes the signal from the transmitter and aid in sending it to both the servo and the speed controller. It is this device that synchronizes to the controller and is what allows the spider robot to receive radio signals as results

of the built-in aerial in the robot. The speed of this controller is the central piece of the research and is what helps in controlling both the servo and the electric motors by regulating their rotation proportional to the amount forced upon it by the transmitter. It is connected to the battery; all of the four motors are in parallel, to the Arduino receiver and a switch. All of the four electric motors are wired in parallel, with two being reverse. This is because there will be two electric motors at either end of the research and when one pair of the leg is walking forward then the other leg needs to be walking backward. By wiring, the motor so current flows in the opposite direction this effect is achieved. With the objective of the spider robot moving forward or backward and avoiding the obstacles on the robot's path. The Arduino board is pre-programmed and waits for the user to input a certain task to be performed. The National Instrument (NI) board helps in collecting feedback information from this sensor embedded on the spider robot frame and processes the information; henceforth, implementing the given job. For instance, if this ultrasonic sensor used senses an item hindering the spider robotic movement route, this sensor will automatically convey the response information to the programmed National Instrument (NI) board. With the help of this board, it will then process the information consequently and evaluates the information to gives a suitable outcome such as enrichment for the location of the spider robot to escape the hitch that leads to self-localization. The spider robot will then start moving onward again till the robot reaches its target or facing another problem on its movement route. The spider robotic program consists of three Digital input and output ports; this includes an ultrasonic sensor, smoke sensor, and temperature sensor. It also consists of four types of walking processes ready to perform singly when this ultrasonic sensor identifies any difficulty in frontage of the spider robot. When there is no difficulty on the spider robot's route, the remaining three of the walking algorithms would not implement. In this case, the only walking algorithm performed is the algorithm for the spider robot moving onward. If this ultrasonic sensor notices a hitch in front of the spider robot, the spider robot will dismiss the walking forward process and then trigger either walking left right or backward walking process. The feedback information that is from the sensor will be performed consequently; henceforth, calling the information that has been made in the memory block to the pulse-width modulated (PWM) generator for each of the servo motors. In this case, when you implement the forward walking procedure, the spider robot limb moves step-by-step. With the six legs of the spider robots taking its respective location, the spider robot will then be able to push its body forward. This procedure will be repeated in order to make a forward movement for the spider robot. The smoke and temperature sensor will perform individually without touching the walking process of the robot. The information that you obtained from both the smoke and temperature sensor is display on your front panel of your monitor. The wireless watching system is an interface on your laptop. On your observing system interface, you can assign a green light emitting diode indicator to represent the direct route taken by the spider robot when the walking process is executed. If in the process the spider robot detects smoke, the red light emitting diode that you assigned to the sensor indicator will light up to signal possible menace. Your surrounding temperature is monitor and updated with the help of indicator thermometer on your laptop or desktop monitoring system.

2.3. Application of the spider robot

1. We can use this spider robot in discovering dangerous or rough areas in which humankind can have full access easily. For example, searching for survivors after a terrible nuclear tragedy, also exploring in war zones, for inspecting unstable buildings after a natural tragedy such as earthquake, tsunami or a volcanic eruption.
2. We can also use spider robots in defusing bombs such as land mines.
3. We can also equip the spider robots with sensors and weapons; such robot is used in a crisis or war to avoid risking human lives on the battlefield.
4. We can also use this spider robot in guarding our properties or areas of high importance.

3. Conclusions

In conclusion, this paper reviewed some studies relating to spider robots, highlighted its principle

of operation, it also summarizes how it is made or constructed and the areas of applications in real life in this world. With the help of advancement in technology, the spider robot system will be able to monitor every important environment also analyzes the situation of such environment in which one can have full access due to the complication of such places and implement the proper action needs to be executed in such areas.

4. REFERENCES

[1] Iborra, A. Pastor, J.A, B. Álvarez, C. Fernández, J.M, Fernández Meroño, 2003. Robots in radioactive environments. "IEEE Robot. Automation". Mag. 10, pp, 12–22. https://doi.org/ 10.1109/MRA.2003.1256294

[2] Cortez, R.A, Papageorgiou, X. H.G, Tanner, A.V, Klimenko, K.N, Borozdin, W.C, Priedhorsky, 2007. Experimental implementation of robotic sequential nuclear search. "Mediterranean Conference on Control and Automation. MED", https://doi.org/10.1109/MED.2007.4433797

[3] Abouaf, J. 1998. Trial by fire: teleoperated robot targets Chernobyl. IEEE Computer. Graph. Appl. 18, pp, 10–14. https://doi.org/10.1109/38.689654.

[4] Bagatin, M. Gerardin, S. Paccagnella, A. 2017. Space and terrestrial radiation effects in Flash memories Radiation effects in recon fi gurable FPGAs. Semicond. Sci. Technol, 32, pp, 1-8

[5] Berry, R. Loebakka, K. E. Hall, 1983. Sensors for mobile robots. "In Proceedings of the 3rd Conference on Robot Vision and Sensory Controls", pp. 584–588.

[6] Bloss, R. 2010. How do you decommission a nuclear installation? "Call in the robots. Ind. Robot An Int". 37, 133–136. https://doi.org/10.1108/01439911011018902

[7] Bogue, R. 2011. Robots in the nuclear industry: a review of technologies and applications. Ind. Robot An Int. J. 38, 113–118. https://doi.org/10.1108/ 01439911111106327

[8] Bradley, D.A, Seward, D.W, 1998. The development, control, and operation of an autonomous robotic excavator. "Intell. Rob", pp, 73–97. https://doi.org/10.1023/ A:1007932011161.

[9] Briones, Bustamante, L. P. Serna, M.A, 1994. Robicen: a wall-climbing pneumatic robot for inspection in nuclear power plants. Robot. Compute, pp287–292. https://doi.org/10.1016/0736-5845(95)00005-4.

[10] Kim, J. H. H. J. Ko, Kim, S. H. Ji, M. G. and Lee, J. B. "Intelligent system of the spider robot for the various moving functions," in Proc. 2009 18th IEEE International Symposium on Robot and Human Interactive Communication (RO-MAN 2009), Toyama, Japan, pp. 226-231.

[11] Ijspeert, A. Central pattern generators for locomotion control in animals and robots: a review, Neural Networks 21 (4) (2008) 642–653.

[12] Cruse, H. D. Brunn, C. Bartling, J. Dean, M. Dreifert, T. Kindermann, Walking: a complex behavior controlled by simple networks, Adaptive Behavior 3 (1995) 385–418.

[13] Figliolini, G. Rea, P. Mechanics, and simulation of six-legged walking robots, in Climbing and Walking Robots Towards New Applications, I-Tech Education and Publishing, Austria, 2007, pp. 1–22.

[14] Autumn, K. Peattie, A. Mechanisms of adhesion in geckos, The Journal of Integrative and Comparative Biology 42 (6) (2002) 1081–1090.

[15] Autumn, K. Sitti, M. Liang, Y. Peattie, A. Hansen, W. Sponberg, S. Kenny, T. R. Fearing, J. Israelachvili, R. Full, Evidence for van der Waals adhesion in gecko setae, Proceedings of the National Academy of Sciences of the USA 99 (19) (2002) 12252–12256.

[16] A. Kesel, A. Martin, T. Seidl, Adhesion measurements on the attachment devices of the jumping spider Evarcha arcuata, Journal of Experimental Biology 206 (2003) 2733–2738.

[17] A. Kesel, A. Martin, T. Seidl, Getting a grip on spider attachment: an AFM approach to microstructure adhesion in arthropods, Smart Materials and Structures 13 (2004) 512–518.

[18] H. Gao, X. Wang, H. Yao, S. Gorb, E. Arzt, Mechanics of hierarchical adhesion structures of geckos, Mechanics of Materials 37 (2–3) (2005) 275–285.

[19] K. Autumn, Y. Liang, S. Hsieh, W. Zesch, W. Chan, T. Kenny, R. Fearing, R. Full,

[20] S. Soyguder and H. Ali. (2012). Kinematic and dynamic analysis of a hexapod walking-running-bounding gaits robot and control actions. Computers and Electrical Engineering, 38(2), pp. 444-458.

[21] Sreerag, R. Muthukumaran, S. B. Sriram, S. John, and B. Thenkalvi, "Tarantula Bot: Rescue Assist Tele Robot," in Proc. 2012 Fourth International Conference on Advanced Computing (ICAC), pp. 1-6.

[22] Tian, W. J. and Geng, Y. "A New Household Security Robot System Based on Wireless Sensor Network," in Proc. 2009 Second International Conference on Future Information Technology and Management Engineering (FITME '09), Sanya, China, pp. 187-190.

[23] Roy, S. S. and Pratihar, D. K. "Dynamic Modeling and Energy Consumption Analysis of Crab Walking of a Six-legged Robot," in Proc. 2011 IEEE Conference on Technologies for Practical Robot Applications (TEPRA), Woburn, Massachusetts, pp. 82-87.

[24] J. A. Cobano, J. Estremera, and P. G. d. Santos. (2010). Accurate tracking of legged robots on natural terrain. Autonomous Robots, 28(2), pp. 231-244.

[25] S. S. Roy, A. K. Singh, and D. K. Pratihar. (2011). Estimation of optimal feet forces and joint torques for on-line control of the six-legged robot. Robotics and Computer-Integrated Manufacturing, 27(5), pp. 910-917.

[26] S. S. Roy and D. K. Pratihar. (2013). Dynamic modeling, stability, and energy consumption analysis of a realistic six-legged walking robot. Robotics and Computer-Integrated Manufacturing, 29(2), pp. 400-416.

[27] Roy, S. S., and Pratihar. D. K. (2012). Effects of turning gait parameters on energy consumption and stability of a six-legged walking robot. Robotics and Autonomous Systems, 60(1), pp. 72-82.

International Journal of New Computer Architectures and their Applications (IJNCAA) 9(1): 25-30
The Society of Digital Information and Wireless Communications, 2019 ISSN 2220-9085 (Online); ISSN 2412-3587 (Print)

Automatic Identification of Plant Physiological Disorders in Plant Factories with Artificial Light Using Convolutional Neural Networks

Shigeharu Shimamura Kenta Uehara Seiichi Koakutsu
Chiba University
1-33, Inage-ku, Yayoi-cho, Chiba-shi 263-8522, Japan
s.shimamura@hanmo.jp

ABSTRACT

Plant factories with artificial light (PFAL) are attracting worldwide attention as a technology for stably producing crops. One of the problems of PFAL is tipburn which is a physiological disorder of crops. Tipburn is a phenomenon in which plant growth point cells are necrotized. Lettuce cultivated in PFAL in particular has a high frequency of tipburn. When tipburn occurs, its identification is done by human eye observation, and tipburn leaves are trimmed by hand or tipburn lettuce is removed from products. These operations require much labor and cost. If tipburn identification can automatically be done using machine learning, the economic effect will be great and it will be a driving force for spreading PFAL. In this study, we aim to perform binary discrimination of tipburn occurrence and its non-occurrence about lettuce cultivated in PFAL using machine learning with convolutional neural networks. In particular, we aim to recognize the symptom of tipburn which means the early stages of tipburn immediately before leaf tips discolor blackly and the commercial value as the vegetables is damaged. The results of the experiments indicate that the recognition of the symptom of tipburn can be performed with high accuracy.

KEYWORDS

machine learning, convolutional neural network, diagnostic imaging, plant factory, plant physiological disorder, tipburn

1 INTRODUCTION

In recent years, smart agriculture, which is a new agriculture that promotes labor-saving and high-quality production by utilizing robot technology, information and communication technology (ICT), and artificial intelligence (AI) technogogy, is regarded as important, because farmers are rapidly aging and labor shortages are becoming serious in Japan's agricultural field. By utilizing smart agriculture, labor saving and lightening can be promoted in farm work, and it is expected to secure new farmers and inherit cultivation technology. In particular, plant factories with artificial light (PFAL) which is one of key technologies for smart agriculture are paid much attention not only in horticuture but also in engineering. PFAL enable to stably produce crops in a closed space where environmental conditions are highly controlled[1].

One of the problems of PFAL is tipburn which is a physiological disorder of crops. In PFAL, the growth of crops is promoted by creating the condition suitable for crops and the period from seeding to harvesting can be reduced, whereas PFAL tends to cause tipburn. Tipburn is a phenomenon in which plant growth point cells are necrotized[2][3][4]. Especially, lettuce cultivated in PFAL has a high frequency of tipburn. When tipburn occurs, leaf tips discolor blackly and the commercial value as vegetables is damaged. Identification of tipburn is done by human eye observation, and tipburn leaves are trimmed by hand or that lettuce is removed from products. These operations require much labor and cost. If tipburn identification can automatically be done using machine learning, economic effect is great and it will be a driving force for spreading PFAL.

Tipburn can be classified into two types, A and B, in case of frill lettuce. Type A tipburn occurs at central leaves, whereas type B tipburn occurs at peripheral ones. Image diagnosis by machine learning using convolutional neural networks (CNNs), which have excellent performance in image recognition, is effective for automatic identification of the occurrence of type A or type B tipburn. We have performed binary discrimination of type B tipburn occurrence and its non-occurrence with accuracy 0.929[5], and binary discrimination of type A tipburn occurrence and its non-occurrence with accuracy 0.986[6] using machine learing with CNNs. The accuracy exceeds target yield (90%) of farm products of PFAL.

In this study, we aim to perform binary discrimination of the symptom of type A tipburn occurrence and its non-occurrence about lettuce cultivated in PFAL using machine learing with CNNs[**?**]. The symptom of tipburn means the early stages of tipburn immediately before leaf tips discolor blackly and the commercial value as vegetables is damaged. Lettuce irreversibly transits from normal to tipburn through a stage of symptom. It is important to detect the symptom of tipburn because lettuce has commercial value and can be sold at the stage of symptom. In addition, we adopt support vector machine (SVM)[7], which is a representative binary discrimination method, as a comparison method, and conduct comparison experiments among various CNN models and SVM. The results of the experiments show that CNNs are effective for binary discrimination of the symptom of type A tipburn occurrence and its non-occurrence.

2 TRAINING DATA

Machine learning requires a large number of training data which include normal lettuce images, symptom ones, and tipburn ones. To obtain the training data, we cultivate normal lettuce, symptom one and tipburn one on purpose. Data labels obtained in this manner are considered highly accurate.

2.1 Test crop and cultivation method

Frill lettuce is one of the crops with the biggest production in PFAL and its economic effect is big. Besides frill lettuce is known as one of crops which have a high frequency of tipburn. Frill ice (Snow Brand Seed Co. LTD.) which is one of frill lettuce is adopted as a test crop.

We adopt two type of PFAL as cultivation systems. One is showcase-type PFAL for normal lettuce, and another is house-type PFAL for symptom one and tipburn one. Both type of PFAL are located at center for environment, health and field sciences in Chiba University. Showcase-type PFAL (HM-PF-DC-AL01, Hanmo Co.) is compact size and easy to control cultivation condition because it installed in an interior and doesnot undergo influence of an outdoor weather fluctuation. House-type PFAL is also easy to control cultivation condition such as temperater and CO_2 level. Temperature and CO_2 level are very imporadant factors to create the clutivation conditions which promote tipburn.

Table 1. System specification (showcase-type FPAL).

♯cultural shelves	3 (seed bed:1, cultivation:2)
controller	lighting cycle, fan control
lighting	white LED (18W) 6
ventilator	8 fans
nutrient solution dispenser	circulator, tank, water level sensor

Table 2. System specification (house-type FPAL).

♯cultural shelves	4
controller	lighting cycle, air conditioner, CO_2 control
lighting	RGB LED (14.5W) 10
nutrient solution dispenser	deep float technique, aeration

Hydroponic culture is adopted as a cultivation method. White LED light in showcase-type FPAL and RGB LED light in house-type FPAL are adopted as artificial lights, because both LED lights contaion wave length which is suitable for photosynthesis, and are low heat generation. In showcase-type PFAL, lighting heat is removed with room air using ventilation fans. In house-type PFAL, air conditoner is used to remove lighting heat and control room air temperature. In addition, CO_2 level is raised in house-type PFAL in order to promote the growth of lettuce and induce tipburn.
Table 1 and 2 show the system specification of showcase-type FPAL and that of house-type FPAL respectively.

2.2 Cultivation condition

In general, tipburn is caused by (1) high temperature, (2) low humidity, (3) high light intensity, (4) long day length, and (5) high nutrient concentration. Parameters for cultivating tipburn lettuce are estimated and tuned in consideration of these factors.

Table 3. Cultivation conditions.

	normal lettuce	tipburn lettuce
cultivation system	showcase-type	house-type
temperature [°C]	18	24
humidity [%]	65∼75	65∼75
day length [h]	L15-D9 (15h)	L20-D4 (20h)
light intensity [μmol/m^2/s]	PPFD200	PPFD200∼250
nutrient concentration [dS/m]	EC1.5	EC2.4

In both type of FPAL, enshi formula nutrient solution which is the most commonly used for hydroponic culture is adopted as nutrient solution.
In showcase-type FPAL, nutrient solution is circulated by a pump from a tank to culture racks 24 hours a day. The flow of nutrient solution is 10 L/min for each culture rack. Ventilation fans operate 18 hous a day. Other conditions are shown in Table 3.
In house-type FPAL, deep float technique with 24-hours aeration is adopted as nutrient solution dispenser. CO_2 level is raised in order to increase photosynthesis and promote growth of lettuce. Liquefied CO_2 gas cylinder is installed in the house-type PFAL, and CO_2 level is controlled to be 2,000 ppm using CO_2 sensor. Other conditions are shown in Table 3.
In Table 3, light intensity is meared with photosynthetic photon flux density (PPFD [μmol/m^2/s]), and nutrient concentration is measured with electrical conductivity (EC [dS/m]).

2.3 Cultivation of lettuce

Lettuce is cultivated as follws. (1) Urethane sheet soaked in tap water is installed in a container designed for raising of seedling, and lettuce seeds are sown there. (2) Lettuce checked on root is transplanted to growing racks three days after sprouting. (3) Lettuce is settled planting in culture racks two weeks after transplant, and cultivated.

2.4 Acquisition of image data

Images of all 24 lettuces are obtaind daily from 35th day after seeding. Indivisual lettuce is checked occurrence or non-occurrence of tipburn by human eye observation, and captured (F/4.0) from above under white lighting and white backgraound with digital camera. Fig. 1 shows an example of normal lettuce, Fig. 2 shows that of symptom of type A tipburn one, and Fig. 3 shows that of type A tipburn one. In Fig. 3, the central leaf tips discolored blackly are tipburn.

3 EXPERIMENTS

We examine binary discrimination of the symptom of type A tipburn occurrence and its non-occurrence about lettuce cultivated in PFAL using machine learning with CNNs. CNNs are suitable for these experiments because CNNs are effective in processing of two-dimensional images.

Figure 1. An example of normal lettuce.

Figure 2. An example of symptom of type A tipburn lettuce.

Figure 3. An example of type A tipburn lettuce.

VGGNet[8], GoogLeNet[9], ResNet[10], and WideResNet[11] are adopted as CNN models. VGGNet is a simple CNN model composed of convolution layers and pooling layers. In VGGNet, a small-scale convolution layer is stacked between the input layer or pooling layers to reduce the number of parameters. Table 4 shows the network structure of VGGNet. GoogLeNet is a CNN model that

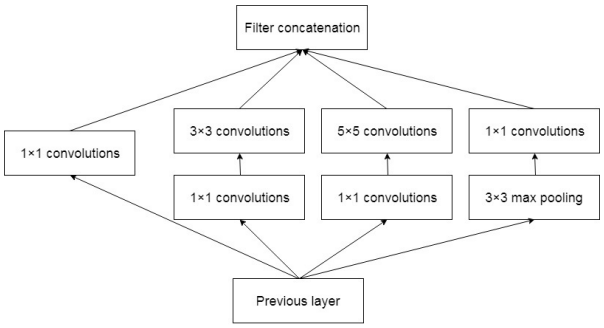

Figure 4. Inception module.

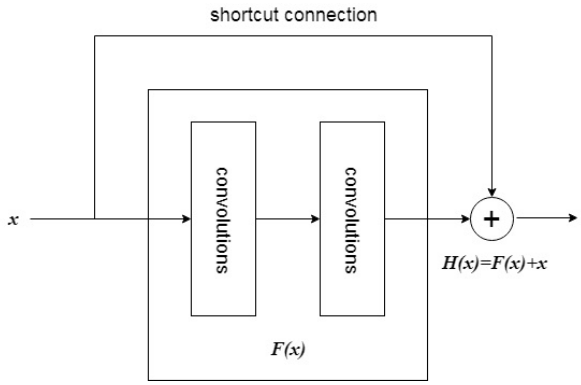

Figure 5. Residual module.

constitutes one large CNN by introducing inception modules in which multiple convolution layers and pooling layers are arranged in parallel, and stacking them like a normal convolution layer. Fig. 4 shows the inception module, and Table 5 shows the network structure of GoogLeNet. ResNet is a CNN model that introduces residual modules. In residual modules, instead of simply passing the transformation $F(x)$ by a processing block to the next layer, the input x to that processing block is shortcut and $H(x) = F(x) + x$ are passed to the next layer. Fig. 5 shows the residual module, and Table 6 shows the network structure of ResNet. WideResNet is a CNN model that increases the input channels of the convolution layer in each residual module instead of deepening the layer in ResNet. Table 7 shows the network structure of WideResNet.

We also examine the same binary discrimination with classical networks in order to exhibit the difficulty of discriminating tipburn lettuce from normal one. Support vector machine (SVM)[7] with histogram of oriented gradients (HOG)[12] is adopted as one of classical networks. SVM is a classifier used in machine learning for the purpose of classification and regression, and HOG is a feature descriptor used in computer vision and image processing for the purpose of object detection. SVM is suitable for our experiments because SVM is effective in binary discrimination.

Table 4. The network structure of VGGNet17

layer	filter	stride	output
input			(224, 224, 3)
convolution×2	(3, 3)	(1, 1)	(224, 224, 64)
max pooling	(2, 2)	(2, 2)	(112, 112, 64)
convolution×2	(3, 3)	(1, 1)	(112, 112, 128)
max pooling	(2, 2)	(2, 2)	(56, 56, 256)
convolution×3	(3, 3)	(1, 1)	(56, 56, 512)
max pooling	(2, 2)	(2, 2)	(28, 28, 512)
convolution×3	(3, 3)	(1, 1)	(28, 28, 512)
max pooling	(2, 2)	(2, 2)	(14, 14, 512)
convolution×3	(3, 3)	(1, 1)	(14, 14, 512)
max pooling	(2, 2)	(2, 2)	(7, 7, 512)
full connected			4096
full connected			4096
full connected			1000
full connected			2

Table 5. The network structure of GoogLeNet22

layer	filter	stride	output
input			(224, 224, 3)
convolution	(7, 7)	(2, 2)	(112, 112, 64)
max pooling	(3, 3)	(2, 2)	(56, 56, 64)
convolution	(3, 3)	(1, 1)	(56, 56, 192)
max pooling	(3, 3)	(2, 2)	(28, 28, 192)
inception×2			(28, 28, 480)
max pooling	(3, 3)	(2, 2)	(14, 14, 480)
inception×5			(14, 14, 832)
max pooling	(3, 3)	(2, 2)	(7, 7, 832)
inception×2			(7, 7, 1024)
avg. pooling	(7, 7)	(1, 1)	(1, 1, 1024)
full connected			256
full connected			2

3.1 Condition

The size of image is 100KB. The number of normal lettuce images, that of symptom ones, and that of tipburn ones are 1200, 1500 and 1100 respectively. GoogLeNet is traind using Adam[13], and the number of training epoch is 50. 90% of image data are used for training, and rest for validation.

3.2 Results

Experimental results are indicated in Table 8 and Fig. 6∼8. Table 8 shows the comparison of various CNN models with SVM in terms of accuacy of test data in case of binary discrimination of normal and tipburn, that of normal and symptom, and that

Table 6. The network structure of ResNet50

layer	filter	stride	output
input			(224, 224, 3)
convolution	(3, 3)	(1, 1)	(224, 224, 17)
residual	$\begin{bmatrix} 1\times1, 17 \\ 3\times3, 4 \\ 1\times1, 17 \end{bmatrix}\times3$	(1, 1)	(224, 224, 17)
residual	$\begin{bmatrix} 1\times1, 17 \\ 3\times3, 8 \\ 1\times1, 32 \end{bmatrix}\times4$	(2, 2)	(112, 112, 32)
residual	$\begin{bmatrix} 1\times1, 32 \\ 3\times3, 17 \\ 1\times1, 64 \end{bmatrix}\times6$	(2, 2)	(56, 56, 64)
residual	$\begin{bmatrix} 1\times1, 64 \\ 3\times3, 32 \\ 1\times1, 128 \end{bmatrix}\times3$	(2, 2)	(28, 28, 128)
avg. pooling	(28, 28)	(1, 1)	(1, 1, 128)
full connected			2

Table 7. The network structure of WideResNet10

layer	filter	stride	output
input			(224, 224, 3)
convolution	(3, 3)	(1, 1)	(224, 224, 17)
residual	$\begin{bmatrix} 3\times3, 17 \\ 3\times3, 48 \end{bmatrix}$	(1, 1)	(224, 224, 48)
residual	$\begin{bmatrix} 3\times3, 48 \\ 3\times3, 96 \end{bmatrix}$	(2, 2)	(112, 112, 96)
residual	$\begin{bmatrix} 3\times3, 96 \\ 3\times3, 192 \end{bmatrix}$	(2, 2)	(56, 56, 192)
residual	$\begin{bmatrix} 3\times3, 192 \\ 3\times3, 384 \end{bmatrix}$	(2, 2)	(28, 28, 384)
avg. pooling	(28, 28)	(1, 1)	(1, 1, 384)
full connected			2

Table 8. Comparison of test accuracy.

	WRN	RN	GN	VGG	SVM
nor.-tipb.	1.000	0.993	0.986	0.977	0.734
nor.-symp.	0.990	0.981	0.977	0.978	0.536
symp.-tipb.	1.000	0.995	0.970	0.870	0.647

of symptom and tipburn respectivly. Fig.6∼8 are examples of learning curves of various CNN models. x-axis indicates learning epochs and y-axis indicates test accuracy.

CNNs are better than SVM in all cases, and test accuracy of CNNs exceeds target yield (90%) of farm products of PFAL in almost all of the cases. Type A tipbarn and its symptom can be recognized with a high degree of accuracy sufficiently using various CNNs.

3.3 Discussion

The results in Table 8 indicate the difficulty of discriminating tipburn lettuce from normal one. The classical network such as SVM cannot distinguish tipburn lettuce from normal one with high degree of accuracy because SVM cannot accurately capture the features of tipburn in the image data.

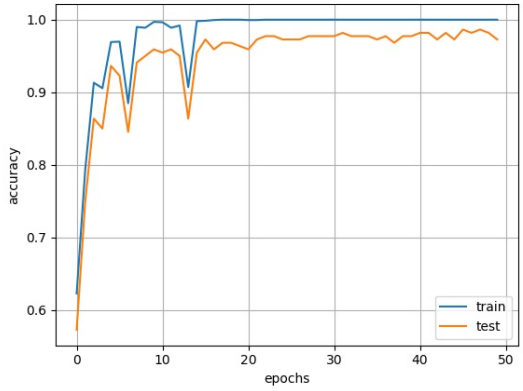

Figure 6. Accuracy (normal-tipburn).

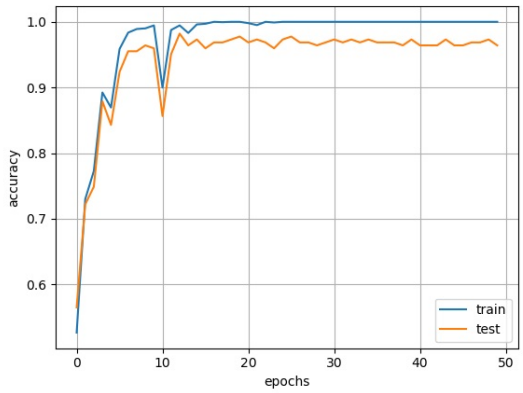

Figure 7. Accuracy (normal-symptom).

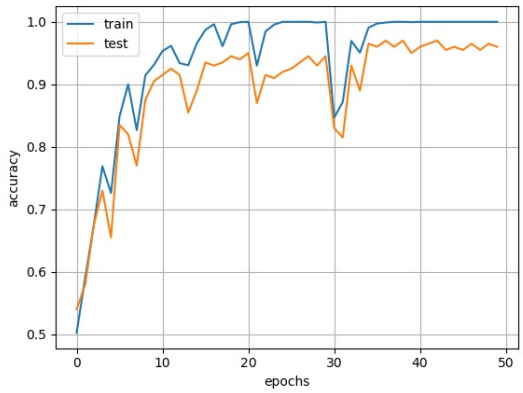

Figure 8. Accuracy (symptom-tipburn).

The results of CNNs indicate binary discrimination of symptom and tipburn is the most difficult, that of normal and symptom is the second most difficult, and that of normal and tipburn is the easyest. The performance of WideResNet is the best, that of

ResNet is the second best, that of GoogLeNet is the third best and VGGNet is the worst.

The reasons of the high degree of accuracy of CNNs are the quality of training image data and the correctness of data labels which indicate normal, symptom, and tipburn. The features of tipburn sufficiently appear in the image data to be captured by CNNs.

The reasons of false recognition of CNNs are described as follows. In case of normal lettuce is falsely recognized with tipburn one, the shadowed area of leaves is falsely recognized with tipburn. On the other hand, in case of tipburn lettuce is falsely recognized with normal one, the features of tipburn in the image data is so slight that CNNs cannot recognise tipburn correctly.

4 CONCLUSION

Binary discrimination of the symptom of type A tipburn occurrence and its non-occurrence could be done by machine learning using CNNs by the high precision as accuracy more than 0.9 about lettuce cultivated in PFAL. It would be commercially meaningful if we could harvest lettuce at the symptom stage of tipburn because lettuce has the commercial value as vegetables at this stage. To test other training algorithms can be future works. Besides in the real PFAL environment, noise on the image, the camera angle and the value of illuminance when the taking a sample photo to recognize should be considered.

REFERENCES

[1] T. Kozai: “Plant Factory with Artificial Light,” pp. 193-212, Ohmsha (2012) (in Japanese).

[2] T. Maruo: “Resarch about Lettuce Tip Burn. (1)Ca Concentration of Individual Lettuce Leaves by Leaf Position,” Hort. Res.(Japan), Vol. 58 (Sppl.2), pp. 193-212 (1983) (in Japanese).

[3] T. Maruo et.al.: “Which Stage the Tip Burn Occurrence Is Determined for Individual Lettuce Leaf?,” Hort. Res.(Japan), Vol. 18 (Sppl.1), pp. 152 (2019) (in Japanese).

[4] E. Goto and T. Takakura: “Reduction of Lettuce Tipburn by Shorting Day/Night Cycle,” J. Agric. Meteorol., Vol. 59, No. 3, pp. 219-225 (2003).

[5] S. Shimamura, K. Uehara, and S. Koakutsu: “Automatic Identification of Plant Physiological Disorders in Plant Factory Crops,” Proc. IEEJ EIS Conf., pp. 1207-1210 (2018) (in Japanese).

[6] S. Shimamura, K. Uehara, and S. Koakutsu: “Automatic Identification of Lettuce Tipburn in Plant Factory Crops,” Proc. Fuzzy, Artificial Intelligence, Neural Networks and Computational Intelligence Symposium (FAN2018), pp. 101-104 (2018) (in Japanese).

[7] I. Tsochantaridis, T. Joachims, T. Hofmann and Y. Altun: “Large Margin Methods for Structured and Interdependent Output Variables,” J. of Machine Learning Research, No.6, pp.1453-1484 (2005).

[8] K. Simonyan and A. Zisserman: “Very Deep Convolutional Networks for Large-scale Image Recognition,” Proc. Int. Conf. on Learning Representations, pp.1-14 (2015).

[9] C. Szegedy, W. Liu, Y. Jia, P. Sermanet, S. Reed, D. Anguelov, D. Erhan, V. Vanhoucke and A. Rabinovich: “Going Deeper with Convolutions,” Proc. IEEE Conf. on Computer Vision and Pattern Recognition, pp. 1-9 (2015).

[10] K. He, X. Zhang, S. Ren and J. Sun: “Deep Residual Learning for Image Recognition,” IEEE Conf. on Computer Vision and Pattern Recognition, pp.770-778 (2016).

[11] S. Zagoruyko and N. Komodakis: “Wide Residual Networks,” arXiv preprint arXiv:1605.07146 (2016).

[12] N. Dalal and B. Triggs: “Histograms of Oriented Gradients for Human Detection,” Proc. IEEE Conf. on Computer Vision and Pattern Recognition, pp.886-893 (2005).

[13] D. P. Kingma and J. L. Ba: “Adam: A Method for Stochastic Optimization,” Proc. Inter. Conf. on Learning Representations, pp. 1-13 (2015).